

APPLICATIONS OF PHYSICS TO ECONOMICS AND FINANCE: MONEY, INCOME, WEALTH, AND THE STOCK MARKET *

Adrian A. Drăgulescu[†]

Department of Physics, University of Maryland, College Park

(Dated: May 15, 2002, cond-mat/0307341)

Abstract: Several problems arising in Economics and Finance are analyzed using concepts and quantitative methods from Physics. The dissertation is organized as follows:

In the first chapter, it is argued that in a closed economic system, money is conserved. Thus, by analogy with energy, the equilibrium probability distribution of money must follow the exponential Boltzmann-Gibbs law characterized by an effective temperature equal to the average amount of money per economic agent. The emergence of Boltzmann-Gibbs distribution is demonstrated through computer simulations of economic models. A thermal machine which extracts a monetary profit can be constructed between two economic systems with different temperatures. The role of debt and models with broken time-reversal symmetry for which the Boltzmann-Gibbs law does not hold, are discussed.

In the second chapter, using data from several sources, it is found that the distribution of income is described for the great majority of population by an exponential distribution, whereas the high-end tail follows a power law. From the individual income distribution, the probability distribution of income for families with two earners is derived and it is shown that it also agrees well with the data. Data on wealth is presented and it is found that the distribution of wealth has a structure similar to the distribution of income. The Lorenz curve and Gini coefficient were calculated and are shown to be in good agreement with both income and wealth data sets.

In the third chapter, the stock-market fluctuations at different time scales are investigated. A model where stock-price dynamics is governed by a geometrical (multiplicative) Brownian motion with stochastic variance is proposed. The corresponding Fokker-Planck equation can be solved exactly. Integrating out the variance, an analytic formula for the time-dependent probability distribution of stock price changes (returns) is found. The formula is in excellent agreement with the Dow-Jones index for the time lags from 1 to 250 trading days. For time lags longer than the relaxation time of variance, the probability distribution can be expressed in a scaling form using a Bessel function. The Dow-Jones data follow the scaling function for seven orders of magnitude.

Contents

Acknowledgements	1	G. Distribution of wealth	15
I. Statistical mechanics of money	2	H. Other distributions for income and wealth	16
A. Introduction	2	I. Conclusions	17
B. Boltzmann-Gibbs distribution	2		
C. Computer simulations	3		
D. Thermal machine	4	III. Distribution of stock-price fluctuations	18
E. Models with debt	4	A. Introduction	18
F. Boltzmann equation	5	B. The model	18
G. Non-Boltzmann-Gibbs distributions	6	C. Solution of the Fokker-Planck equation	19
H. Nonlinear Boltzmann equation vs. linear master equation	7	D. Path-Integral Solution	20
I. Conclusions	7	E. Averaging over variance	20
II. Distribution of income and wealth	8	F. Asymptotic behavior for long time t	21
A. Introduction	8	G. Asymptotic behavior for large log-return x	23
B. Distribution of income for individuals	8	H. Comparison with Dow-Jones time series	24
C. Exponential distribution of income	8	I. Conclusions	25
D. Power-law tail and “Bose” condensation	10		
E. Geographical variations in income distribution	11		
F. Distribution of income for families	13		
		IV. Path-integral solution of the Cox-Ingersoll-Ross/Feller model	26
		References	29
		Acknowledgements	

*This document is a reformatted version of my PhD thesis. Advisor: Professor Victor M. Yakovenko. Committee: Professor J. Robert Dorfman, Professor Theodore L. Einstein, Professor Bei-Lok Hu, and Professor John D. Weeks.

My six year apprenticeship in physics at the University of Maryland was a unique and remarkable leg of my life. And to a large degree this is due to my advisor, Professor Victor M. Yakovenko, who has been at the center of my PhD education. I will deeply miss his clear perspective, his sure hand, and the incommensurate thrill of doing physics together.

I am grateful to Professors J. Robert Dorfman, Theodore L. Einstein, Bei-Lok Hu, and John D. Weeks for agreeing to serve on my advisory committee.

Thanks are also due to Krishnendu Sengupta, Nicholas Dupuis, Hyok-Jon Kwon, Anatole Zheleznyak, and Hsi-Sheng Goan all former students or post-docs of professor Victor Yakovenko, for stimulating discussions in condensed matter physics. My interests in physics were greatly molded by professor Bei-Lok Hu, through his remarkable courses in non-equilibrium physics, and also through personal interaction for more than three years. I had profited a lot from the association with Charis Anastopoulos and Sanjiv Shresta while working on quantum optics problems suggested by professor Bei-Lok Hu.

It is not without melancholy that I thank my first true physics teachers: Ion Cotăescu, Ovidiu Lipan, Dan Luca, Adrian Neagu, Mircea Raşa, Costel Raşinariu, Vlad Socoliu, and Dumitru Vulcanov. On an even deeper layer, I thank my family for all the support they provided me over the years, and for allowing me to pursue my interests.

All the people mentioned above have generously shared with me some of their time and knowledge. I will do all I can to represent them well.

I. STATISTICAL MECHANICS OF MONEY

A. Introduction

The application of statistical physics methods to economics promises fresh insights into problems traditionally not associated with physics (see, for example, the recent review and book¹). Both statistical mechanics and economics study big ensembles: collections of atoms or economic agents, respectively. The fundamental law of equilibrium statistical mechanics is the Boltzmann-Gibbs law, which states that the probability distribution of energy ε is $P(\varepsilon) = Ce^{-\varepsilon/T}$, where T is the temperature, and C is a normalizing constant². The main ingredient that is essential for the textbook derivation of the Boltzmann-Gibbs law² is the conservation of energy³. Thus, one may generalize that any conserved quantity in a big statistical system should have an exponential probability distribution in equilibrium.

An example of such an unconventional Boltzmann-Gibbs law is the probability distribution of forces experienced by the beads in a cylinder pressed with an external force⁴. Because the system is at rest, the total force along the cylinder axis experienced by each layer of granules is constant and is randomly distributed among the individual beads. Thus the conditions are satisfied for the applicability of the Boltzmann-Gibbs law to the force, rather than energy, and it was indeed found experimentally⁴.

We claim that, in a closed economic system, the total amount of money is conserved. Thus the equilibrium probability distribution of money $P(m)$ should follow the Boltzmann-Gibbs law $P(m) = Ce^{-m/T}$. Here m is money, and T is an effective temperature equal to the average amount of money per economic agent. The conservation law of

money⁵ reflects their fundamental property that, unlike material wealth, money (more precisely the fiat, “paper” money) is not allowed to be manufactured by regular economic agents, but can only be transferred between agents. Our approach here is very similar to that of Ispolatov *et al.*⁶. However, they considered only models with broken time-reversal symmetry, for which the Boltzmann-Gibbs law typically does not hold. The role of time-reversal symmetry and deviations from the Boltzmann-Gibbs law are discussed in detail in Sec. I.G.

It is tempting to identify the money distribution $P(m)$ with the distribution of wealth⁶. However, money is only one part of wealth, the other part being material wealth. Material products have no conservation law because they can be manufactured, destroyed, consumed, etc. Moreover, the monetary value of a material product (the price) is not constant. The same applies to stocks, which economics textbooks explicitly exclude from the definition of money⁷. So, we do not expect the Boltzmann-Gibbs law for the distribution of wealth. Some authors believe that wealth is distributed according to a power law (Pareto-Zipf), which originates from a multiplicative random process⁸. Such a process may reflect, among other things, the fluctuations of prices needed to evaluate the monetary value of material wealth.

B. Boltzmann-Gibbs distribution

Let us consider a system of many economic agents $N \gg 1$, which may be individuals or corporations. In this thesis, we only consider the case where their number is constant. Each agent i has some money m_i and may exchange it with other agents. It is implied that money is used for some economic activity, such as buying or selling material products; however, we are not interested in that aspect. As in Ref.⁶, for us the only result of interaction between agents i and j is that some money Δm changes hands: $[m_i, m_j] \rightarrow [m'_i, m'_j] = [m_i - \Delta m, m_j + \Delta m]$. Notice that the total amount of money is conserved in each transaction: $m_i + m_j = m'_i + m'_j$. This local conservation law of money⁵ is analogous to the conservation of energy in collisions between atoms. We assume that the economic system is closed, i. e. there is no external flux of money, thus the total amount of money M in the system is conserved. Also, in the first part of this chapter, we do not permit any debt, so each agent’s money must be non-negative: $m_i \geq 0$. A similar condition applies to the kinetic energy of atoms: $\varepsilon_i \geq 0$.

Let us introduce the probability distribution function of money $P(m)$, which is defined so that the number of agents with money between m and $m + dm$ is equal to $NP(m) dm$. We are interested in the stationary distribution $P(m)$ corresponding to the state of thermodynamic equilibrium. In this state, an individual agent’s money m_i strongly fluctuates, but the overall probability distribution $P(m)$ does not change.

The equilibrium distribution function $P(m)$ can be derived in the same manner as the equilibrium distribution function of energy $P(\varepsilon)$ in physics². Let us divide the system into two subsystems 1 and 2. Taking into account that money is conserved and additive: $m = m_1 + m_2$, whereas the

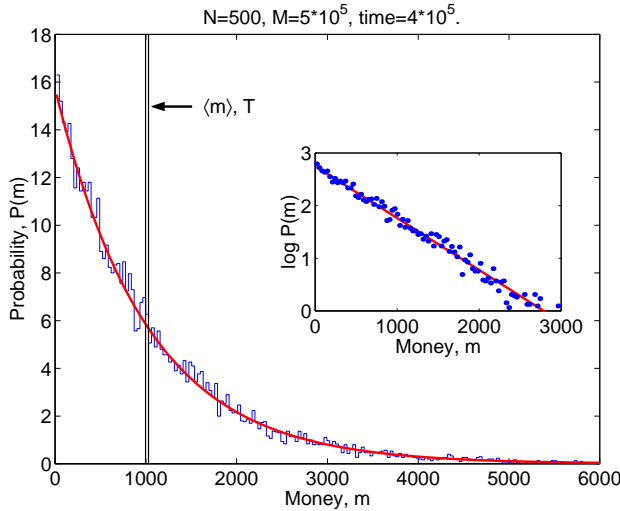


FIG. 1: Histogram and points: stationary probability distribution of money $P(m)$. Solid curves: fits to the Boltzmann-Gibbs law $P(m) \propto \exp(-m/T)$. Vertical lines: the initial distribution of money.

probability is multiplicative: $P = P_1 P_2$, we conclude that $P(m_1 + m_2) = P(m_1)P(m_2)$. The solution of this equation is $P(m) = Ce^{-m/T}$; thus the equilibrium probability distribution of money has the Boltzmann-Gibbs form. From the normalization conditions $\int_0^\infty P(m) dm = 1$ and $\int_0^\infty m P(m) dm = M/N$, we find that $C = 1/T$ and $T = M/N$. Thus, the effective temperature T is the average amount of money per agent.

The Boltzmann-Gibbs distribution can be also derived by maximizing the entropy of money distribution $S = -\int_0^\infty dm P(m) \ln P(m)$ under the constraint of money conservation². Following original Boltzmann's argument, let us divide the money axis $0 \leq m \leq \infty$ into small bins of size dm and number the bins consecutively with the index $b = 1, 2, \dots$. Let us denote the number of agents in a bin b as N_b , the total number being $N = \sum_{b=1}^\infty N_b$. The agents in the bin b have money m_b , and the total money is $M = \sum_{b=1}^\infty m_b N_b$. The probability of realization of a certain set of occupation numbers $\{N_b\}$ is proportional to the number of ways N agents can be distributed among the bins preserving the set $\{N_b\}$. This number is $N! / N_1! N_2! \dots$. The logarithm of probability is entropy $\ln N! - \sum_{b=1}^\infty \ln N_b!$. When the numbers N_b are big and Stirling's formula $\ln N! \approx N \ln N - N$ applies, the entropy per agent is $S = (N \ln N - \sum_{b=1}^\infty N_b \ln N_b)/N = -\sum_{b=1}^\infty P_b \ln P_b$, where $P_b = N_b/N$ is the probability that an agent has money m_b . Using the method of Lagrange multipliers to maximize the entropy S with respect to the occupation numbers $\{N_b\}$ with the constraints on the total money M and the total number of agents N generates the Boltzmann-Gibbs distribution for $P(m)$ ².

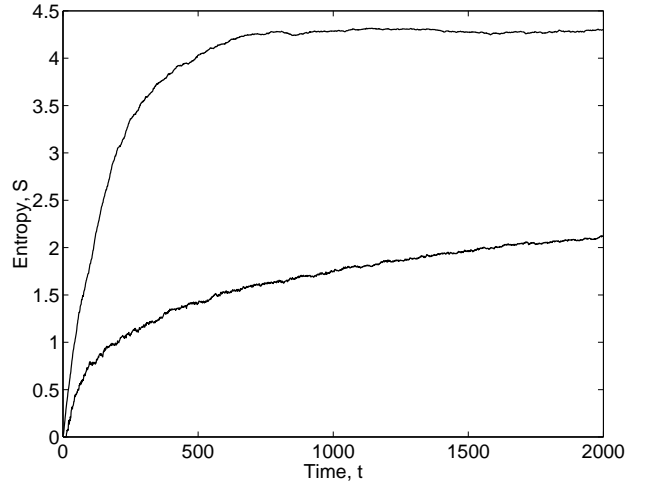


FIG. 2: Time evolution of entropy. Top curve: for the exchange of a random fraction ν of the average money in the system: $\Delta m = \nu M/N$. Bottom curve: for the exchange of a small constant amount $\Delta m = 1$. The time scale for the bottom curve is 500 times greater than indicated, so it actually ends at the time 10^6 .

C. Computer simulations

To check that these general arguments indeed work, we performed several computer simulations. Initially, all agents are given the same amount of money: $P(m) = \delta(m - M/N)$, which is shown in Fig. 1 as the double vertical line. One pair of agents at a time is chosen randomly, then one of the agents is randomly picked to be the “winner” (the other agent becomes the “loser”), and the amount $\Delta m \geq 0$ is transferred from the loser to the winner. If the loser does not have enough money to pay ($m_i < \Delta m$), then the transaction does not take place, and we proceed to another pair of agents. Thus, the agents are not permitted to have negative money. This boundary condition is crucial in establishing the stationary distribution. As the agents exchange money, the initial delta-function distribution first spreads symmetrically. Then, the probability density starts to pile up at the impenetrable boundary $m = 0$. The distribution becomes asymmetric (skewed) and ultimately reaches the stationary exponential shape shown in Fig. 1. We used several trading rules in the simulations: the exchange of a small constant amount $\Delta m = 1$, the exchange of a random fraction $0 \leq \nu \leq 1$ of the average money of the pair: $\Delta m = \nu(m_i + m_j)/2$, and the exchange of a random fraction ν of the average money in the system: $\Delta m = \nu M/N$. Figures in this chapter mostly show simulations for the third rule; however, the final stationary distribution was found to be the same for all rules.

In the process of evolution, the entropy S of the system increases in time and saturates at the maximal value for the Boltzmann-Gibbs distribution. This is illustrated by the top curve in Fig. 2 computed for the third rule of exchange. The bottom curve in Fig. 2 shows the time evolution of entropy for the first rule of exchange. The time scale for this curve is 500 times greater than for the top curve, so the bottom curve

actually ends at the time 10^6 . The plot shows that, for the first rule of exchange, mixing is much slower than for the third one. Nevertheless, even for the first rule, the system also eventually reaches the Boltzmann-Gibbs state of maximal entropy, albeit over a time much longer than shown in Fig. 2.

One might argue that the pairwise exchange of money may correspond to a medieval market, but not to a modern economy. In order to make the model somewhat more realistic, we introduce firms. One agent at a time becomes a “firm”. The firm borrows capital K from another agent and returns it with an interest rK , hires L agents and pays them wages W , manufactures Q items of a product and sells it to Q agents at a price R . All of these agents are randomly selected. The firm receives the profit $F = RQ - LW - rK$. The net result is a many-body exchange of money that still satisfies the conservation law.

Parameters of the model are selected following the procedure described in economics textbooks⁷. The aggregate demand-supply curve for the product is taken to be $R(Q) = V/Q^\eta$, where Q is the quantity people would buy at a price R , and $\eta = 0.5$ and $V = 100$ are constants. The production function of the firm has the conventional Cobb-Douglas form: $Q(L, K) = L^\beta K^{1-\beta}$, where $\beta = 0.8$ is a constant. In our simulation, we set $W = 10$. By maximizing firm’s profit F with respect to K and L , we find the values of the other parameters: $L = 20$, $Q = 10$, $R = 32$, and $F = 68$.

However, the actual values of the parameters do not matter. Our computer simulations show that the stationary probability distribution of money in this model always has the universal Boltzmann-Gibbs form independent of the model parameters.

D. Thermal machine

As explained in the Introduction, the money distribution $P(m)$ should not be confused with the distribution of wealth. We believe that $P(m)$ should be interpreted as the instantaneous distribution of purchasing power in the system. Indeed, to make a purchase, one needs money. Material wealth normally is not used directly for a purchase. It needs to be sold first to be converted into money.

Let us consider an outside monopolistic vendor selling a product (say, cars) to the system of agents at a price p . Suppose that a certain small fraction f of the agents needs to buy the product at a given time, and each agent who has enough money to afford the price will buy one item. The fraction f is assumed to be sufficiently small, so that the purchase does not perturb the whole system significantly. At the same time, the absolute number of agents in this group is assumed to be big enough to make the group statistically representative and characterized by the Boltzmann-Gibbs distribution of money. The agents in this group continue to exchange money with the rest of the system, which acts as a thermal bath. The demand for the product is constantly renewed, because products purchased in the past expire after a certain time. In this situation, the vendor can sell the product persistently, thus creating a small steady leakage of money from the system to the vendor.

What price p would maximize the vendor’s income?

To answer this question, it is convenient to introduce the cumulative distribution of purchasing power $\mathcal{N}(m) = N \int_m^\infty P(m') dm' = Ne^{-m/T}$, which gives the number of agents whose money is greater than m . The vendor’s income is $fp\mathcal{N}(p)$. It is maximal when $p = T$, i. e. the optimal price is equal to the temperature of the system. This conclusion also follows from the simple dimensional argument that temperature is the only money scale in the problem. At the price $p = T$ that maximizes the vendor’s income, only the fraction $\mathcal{N}(T)/N = e^{-1} = 0.37$ of the agents can afford to buy the product.

Now let us consider two disconnected economic systems, one with the temperature T_1 and another with T_2 : $T_1 > T_2$. A vendor can buy a product in the latter system at its equilibrium price T_2 and sell it in the former system at the price T_1 , thus extracting the speculative profit $T_1 - T_2$, as in a thermal machine. This example suggests that speculative profit is possible only when the system as a whole is out of equilibrium. As money is transferred from the high- to the low-temperature system, their temperatures become closer and eventually equal. After that, no speculative profit is possible, which would correspond to the “thermal death” of the economy. This example brings to mind economic relations between developed and developing countries, with manufacturing in the poor (low-temperature) countries for export to the rich (high-temperature) ones.

We will demonstrate in Ch. II that for the large majority of the population the distribution of income is exponential. Hence, similar to the distribution of money, the distribution of income has a corresponding temperature. If in the previous discussion about economic trade, the two countries have a different temperature for the distribution of income, the possibility of constructing a thermal machine will still hold true. This is because purchasing power (total money) per unit time has two components: a positive one, income and a negative one, spending. Instead of making a one time purchase, the buyer will buy one product per unit time, effectively creating the thermal engine. We will revisit this idea in Sec. II E when we give the values for income temperature between the states of the USA and for the United Kingdom.

E. Models with debt

Now let us discuss what happens if the agents are permitted to go into debt. Debt can be viewed as negative money. Now when a loser does not have enough money to pay, he can borrow the required amount from a reservoir, and his balance becomes negative. The conservation law is not violated: The sum of the winner’s positive money and loser’s negative money remains constant. When an agent with a negative balance receives money as a winner, she uses this money to repay the debt until her balance becomes positive. We assume for simplicity that the reservoir charges no interest for the lent money. However, because it is not sensible to permit unlimited debt, we put a limit m_d on the maximal debt of an agent: $m_i > -m_d$. This new boundary condition $P(m < -m_d) = 0$ replaces the old boundary condition

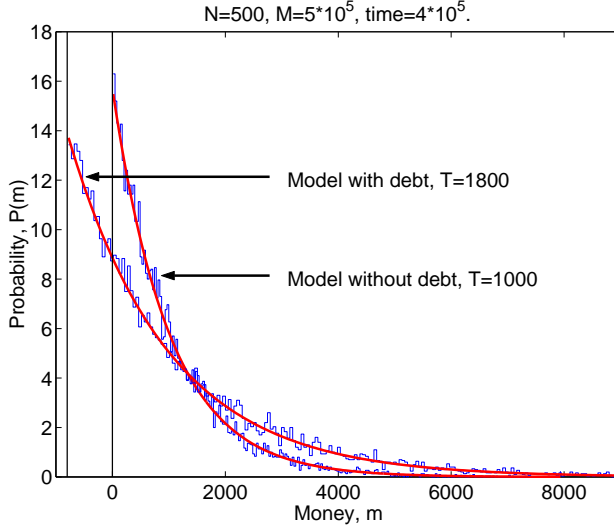


FIG. 3: Histograms: stationary distributions of money with and without debt. Solid curves: fits to the Boltzmann-Gibbs laws with temperatures $T = 1800$ and $T = 1000$.

$P(m < 0) = 0$. The result of a computer simulation with $m_d = 800$ is shown in Fig. 3 together with the curve for $m_d = 0$. $P(m)$ is again given by the Boltzmann-Gibbs law, but now with the higher temperature $T = M/N + m_d$, because the normalization conditions need to be maintained including the population with negative money: $\int_{-m_d}^{\infty} P(m) dm = 1$ and $\int_{-m_d}^{\infty} m P(m) dm = M/N$. The higher temperature makes the money distribution broader, which means that debt increases inequality between agents.

In general, temperature is completely determined by the average money per agent, $\langle m \rangle = M/N$, and the boundary conditions. Suppose the agents are required to have no less money than m_1 and no more than m_2 : $m_1 \leq m \leq m_2$. In this case, the two normalization conditions: $\int_{m_1}^{m_2} P(m) dm = 1$ and $\int_{m_1}^{m_2} m P(m) dm = \langle m \rangle$ with $P(m) = C e^{-m/T}$ give the following equation for T

$$\coth\left(\frac{\Delta m}{T}\right) - \frac{T}{\Delta m} = \frac{\bar{m} - \langle m \rangle}{\Delta m}, \quad (1)$$

where $\bar{m} = (m_1 + m_2)/2$ and $\Delta m = (m_2 - m_1)/2$. It follows from Eq. (1) that the temperature is positive when $\bar{m} > \langle m \rangle$, negative when $\bar{m} < \langle m \rangle$, and infinite ($P(m) = \text{const}$) when $\bar{m} = \langle m \rangle$. In particular, if agents' money are bounded from above, but not from below: $-\infty \leq m \leq m_2$, the temperature is negative. That means an inverted Boltzmann-Gibbs distribution with more rich agents than poor.

Imposing a sharp cutoff at m_d may be not quite realistic. In practice, the cutoff may be extended over some range depending on the exact bankruptcy rules. Over this range, the Boltzmann-Gibbs distribution would be smeared out. So we expect to see the Boltzmann-Gibbs law only sufficiently far from the cutoff region. Similarly, in experiment⁴, some deviations from the exponential law were observed near the lower boundary of the distribution. Also, at the high end of the dis-

tributions, the number of events becomes small and statistics poor, so the Boltzmann-Gibbs law loses applicability. Thus, we expect the Boltzmann-Gibbs law to hold only for the intermediate range of money not too close either to the lower boundary or to the very high end. However, this range is the most relevant, because it covers the great majority of population.

Lending creates equal amounts of positive (asset) and negative (liability) money^{5,7}. When economics textbooks describe how “banks create money” or “debt creates money”⁷, they do not count the negative liabilities as money, and thus their money is not conserved. In our operational definition of money, we include all financial instruments with fixed denomination, such as currency, IOUs, and bonds, but not material wealth or stocks, and we count both assets and liabilities. With this definition, money is conserved, and we expect to see the Boltzmann-Gibbs distribution in equilibrium. Unfortunately, because this definition differs from economists’ definitions of money (M1, M2, M3, etc.⁷), it is not easy to find the appropriate statistics. Of course, money can be also emitted by a central bank or government. This is analogous to an external influx of energy into a physical system. However, if this process is sufficiently slow, the economic system may be able to maintain quasi-equilibrium, characterized by a slowly changing temperature.

We performed a simulation of a model with one bank and many agents. The agents keep their money in accounts on which the bank pays interest. The agents may borrow money from the bank, for which they must pay interest in monthly installments. If they cannot make the required payments, they may be declared bankrupt, which relieves them from the debt, but the liability is transferred to the bank. In this way, the conservation of money is maintained. The model is too elaborate to describe it in full detail here. We found that, depending on the parameters of the model, either the agents constantly lose money to the bank, which steadily reduces the agents’ temperature, or the bank constantly loses money, which drives down its own negative balance and steadily increases the agents’ temperature.

F. Boltzmann equation

The Boltzmann-Gibbs distribution can be also derived from the Boltzmann equation⁹, which describes the time evolution of the distribution function $P(m)$ due to pairwise interactions:

$$\frac{dP(m)}{dt} = \iint \{-w_{[m,m'] \rightarrow [m-\Delta,m'+\Delta]} P(m)P(m') + w_{[m-\Delta,m'+\Delta] \rightarrow [m,m']} P(m-\Delta)P(m'+\Delta)\} dm' d\Delta. \quad (2)$$

Here $w_{[m,m'] \rightarrow [m-\Delta,m'+\Delta]}$ is the rate of transferring money Δ from an agent with money m to an agent with money m' . If a model has time-reversal symmetry, then the transition rate of a direct process is the same as the transition rate of the reversed process, thus the w -factors in the first and second lines of Eq. (2) are equal. In this case, it can be easily checked that the Boltzmann-Gibbs distribution $P(m) = C \exp(-m/T)$

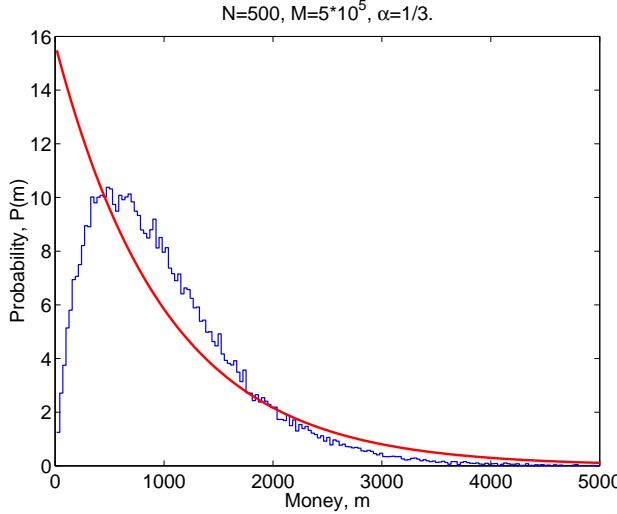


FIG. 4: Histogram: stationary probability distribution of money in the multiplicative random exchange model studied in Ref.⁶. Solid curve: the Boltzmann-Gibbs law.

nullifies the right-hand side of Eq. (2); thus this distribution is stationary: $dP(m)/dt = 0^9$.

G. Non-Boltzmann-Gibbs distributions

However, if time-reversal symmetry is broken, the two transition rates w in Eq. (2) may be different, and the system may have a non-Boltzmann-Gibbs stationary distribution or no stationary distribution at all. Examples of this kind were studied in Ref.⁶. One model was called multiplicative random exchange. In this model, a randomly selected loser i loses a fixed fraction α of his money m_i to a randomly selected winner j : $[m_i, m_j] \rightarrow [(1 - \alpha)m_i, m_j + \alpha m_i]$. If we try to reverse this process and immediately appoint the winner j to become a loser, the system does not return to the original configuration $[m_i, m_j]$: $[(1 - \alpha)m_i, m_j + \alpha m_i] \rightarrow [(1 - \alpha)m_i + \alpha(m_j + \alpha m_i), (1 - \alpha)(m_j + \alpha m_i)]$. Except for $\alpha = 1/2$, the exponential distribution function is not a stationary solution of the Boltzmann equation derived for this model in Ref.⁶. Instead, the stationary distribution has the shape shown in Fig. 4 for $\alpha = 1/3$, which we reproduced in our numerical simulations. It still has an exponential tail end at the high end, but drops to zero at the low end for $\alpha < 1/2$. Another example of similar kind was studied in Ref.¹⁰, which appeared after the first version of our paper was posted as cond-mat/0001432 on January 30, 2000. In that model, the agents save a fraction λ of their money and exchange a random fraction ϵ of their total remaining money: $[m_i, m_j] \rightarrow [\lambda m_i + \epsilon(1 - \lambda)(m_i + m_j), \lambda m_j + (1 - \epsilon)(1 - \lambda)(m_i + m_j)]$. This exchange also does not return to the original configuration after being reversed. The stationary probability distribution was found in Ref.¹⁰ to be nonexponential for $\lambda \neq 0$ with a shape qualitatively similar to the one shown in Fig. 4.

Another interesting example which has a non-Boltzmann-

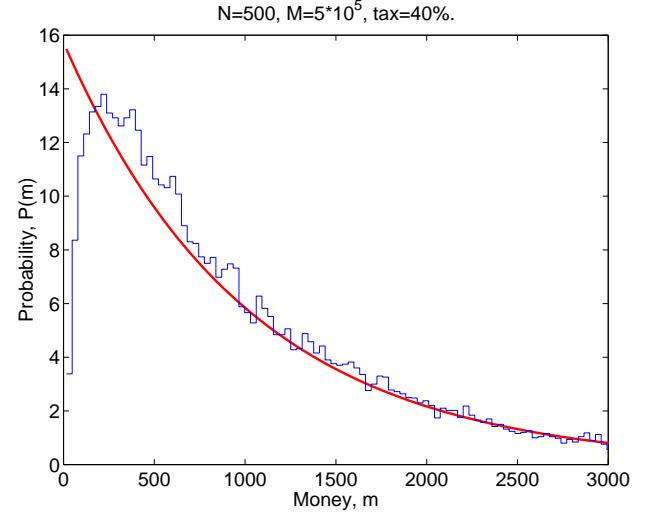


FIG. 5: Histogram: stationary probability distribution of money in the model with taxes and subsidies. Solid curve: the Boltzmann-Gibbs law.

Gibbs distribution occurs in a model with taxes and subsidies. Suppose a special agent (“government”) collects a fraction (“tax”) of every transaction in the system. The collected money is then equally divided among all agents of the system, so that each agent receives the subsidy δm with the frequency $1/\tau_s$. Assuming that δm is small and approximating the collision integral with a relaxation time τ_r ⁹, we obtain the following Boltzmann equation

$$\frac{\partial P(m)}{\partial t} + \frac{\delta m}{\tau_s} \frac{\partial P(m)}{\partial m} = -\frac{P(m) - \tilde{P}(m)}{\tau_r}, \quad (3)$$

where $\tilde{P}(m)$ is the equilibrium Boltzmann-Gibbs function. The second term in the left-hand side of Eq. (3) is analogous to the force applied to electrons in a metal by an external electric field⁹. The approximate stationary solution of Eq. (3) is the displaced Boltzmann-Gibbs one: $P(m) = \tilde{P}(m - (\tau_r/\tau_s)\delta m)$. The displacement of the equilibrium distribution $\tilde{P}(m)$ by $(\tau_r/\tau_s)\delta m$ would leave an empty gap near $m = 0$. This gap is filled by interpolating between zero population at $m = 0$ and the displaced distribution. The curve obtained in a computer simulation of this model (Fig. 5) qualitatively agrees with this expectation. The low-money population is suppressed, because the government, acting as an external force, “pumps out” that population and pushes the system out of thermodynamic equilibrium. We found that the entropy of the stationary state in the model with taxes and subsidies is few a percent lower than without.

These examples show that the Boltzmann-Gibbs distribution is not fully universal, meaning that it does not hold for just any model of exchange that conserves money. Nevertheless, it is universal in a limited sense: For a broad class of models that have time-reversal symmetry, the stationary distribution is exponential and does not depend on the details of a model. Conversely, when time-reversal symmetry is broken, the distribution may depend on model details. The dif-

ference between these two classes of models may be rather subtle. For example, let us change the multiplicative random exchange from a fixed fraction of loser's money to a fixed fraction of the total money of winner and loser. This modification retains the multiplicative idea that the amount exchanged is proportional to the amount involved, but restores time-reversal symmetry and the Boltzmann-Gibbs distribution. In the model with $\Delta m = 1$ discussed in the next Section, the difference between time-reversible and time-irreversible formulations amounts to the difference between impenetrable and absorbing boundary conditions at $m = 0$. Unlike in physics, in economy there is no fundamental requirement that interactions have time-reversal symmetry. However, in the absence of detailed knowledge of real microscopic dynamics of economic exchange, the semiuniversal Boltzmann-Gibbs distribution appears to be a natural starting point.

Moreover, deviations from the Boltzmann-Gibbs law may occur only if the transition rates w in Eq. (2) explicitly depend on the agents' money m or m' in an asymmetric manner. In another simulation, we randomly preselected winners and losers for every pair of agents (i, j) . In this case, money flows along directed links between the agents: $i \rightarrow j \rightarrow k$, and time-reversal symmetry is strongly broken. This model is closer to the real economy, in which, for example, one typically receives money from an employer and pays it to a grocer, but rarely the reverse. Nevertheless, we still found the Boltzmann-Gibbs distribution of money in this model, because the transition rates w do not explicitly depend on m and m' .

H. Nonlinear Boltzmann equation vs. linear master equation

For the model where agents randomly exchange the constant amount $\Delta m = 1$, the Boltzmann equation is:

$$\begin{aligned} \frac{dP_m}{dt} &= P_{m+1} \sum_{n=0}^{\infty} P_n + P_{m-1} \sum_{n=1}^{\infty} P_n \\ &\quad - P_m \sum_{n=0}^{\infty} P_n - P_m \sum_{n=1}^{\infty} P_n \quad (4) \\ &= (P_{m+1} + P_{m-1} - 2P_m) + P_0(P_m - P_{m-1}), \quad (5) \end{aligned}$$

where $P_m \equiv P(m)$ and we have used $\sum_{m=0}^{\infty} P_m = 1$. The first, diffusion term in Eq. (5) is responsible for broadening of the initial delta-function distribution. The second term, proportional to P_0 , is essential for the Boltzmann-Gibbs distribution $P_m = e^{-m/T}(1 - e^{-1/T})$ to be a stationary solution of Eq. (5). In a similar model studied in Ref.⁶, the second term was omitted on the assumption that agents who lost all money are eliminated: $P_0 = 0$. In that case, the total number of agents is not conserved, and the system never reaches any stationary distribution. Time-reversal symmetry is violated, since transitions into the state $m = 0$ are permitted, but not out of this state.

If we treat P_0 as a constant, Eq. (5) looks like a linear Fokker-Planck equation⁹ for P_m , with the first term describing diffusion and the second term an external force proportional

to P_0 . Similar equations were studied in Ref.⁸. Eq. (5) can be also rewritten as

$$\frac{dP_m}{dt} = P_{m+1} - (2 - P_0)P_m + (1 - P_0)P_{m-1}. \quad (6)$$

The coefficient $(1 - P_0)$ in front of P_{m-1} represents the rate of increasing money by $\Delta m = 1$, and the coefficient 1 in front of P_{m+1} represents the rate of decreasing money by $\Delta m = -1$. Since $P_0 > 0$, the former is smaller than the latter, which results in the stationary Boltzmann-Gibbs distributions $P_m = (1 - P_0)^m$. An equation similar to Eq. (6) describes a Markov chain studied for strategic market games in Ref.¹¹. Naturally, the stationary probability distribution of wealth in that model was found to be exponential¹¹.

Even though Eqs. (5) and (6) look like linear equations, nevertheless the Boltzmann equation (2) and (4) is a profoundly nonlinear equation. It contains the product of two probability distribution functions P in the right-hand side, because two agents are involved in money exchange. Most studies of wealth distribution⁸ have the fundamental flaw that they use a single-particle approach. They assume that the wealth of an agent may change just by itself and write a linear master equation for the probability distribution. Because only one particle is considered, this approach cannot adequately incorporate conservation of money. In reality, an agent can change money only by interacting with another agent, thus the problem requires a two-particle probability distribution function. Using Boltzmann's molecular chaos hypothesis, the two-particle function is factorized into a product of two single-particle distributions functions, which results in the nonlinear Boltzmann equation. Conservation of money is adequately incorporated in this two-particle approach, and the universality of the exponential Boltzmann-Gibbs distribution is transparent.

I. Conclusions

Everywhere in this chapter we assumed some randomness in the exchange of money. Our results would apply the best to the probability distribution of money in a closed community of gamblers. In more traditional economic studies, the agents exchange money not randomly, but following deterministic strategies, such as maximization of utility functions^{5,12}. The concept of equilibrium in these studies is similar to mechanical equilibrium in physics, which is achieved by minimizing energy or maximizing utility. However, for big ensembles, statistical equilibrium is a more relevant concept. When many heterogeneous agents deterministically interact and spend various amounts of money from very little to very big, the money exchange is effectively random. In the future, we would like to uncover the Boltzmann-Gibbs distribution of money in a simulation of a big ensemble of economic agents following realistic deterministic strategies with money conservation taken into account. That would be the economics analog of molecular dynamics simulations in physics. While atoms collide following fully deterministic equations of motion, their energy exchange is effectively random due to the complexity of the system and results in the Boltzmann-Gibbs law.

We do not claim that the real economy is in equilibrium. (Most of the physical world around us is not in true equilibrium either.) Nevertheless, the concept of statistical equilibrium is a very useful reference point for studying nonequilibrium phenomena.

II. DISTRIBUTION OF INCOME AND WEALTH

A. Introduction

In Ch. I we predicted that the distribution of money should follow an exponential Boltzmann-Gibbs law. Unfortunately, we were not able to find data on the distribution of money. On the other hand, we found many sources with data on income distribution for the United States (USA) and United Kingdom (UK), as well as data on the wealth distribution in the UK, which are presented in this chapter. In all of these data, we find that the great majority of the population is described by an exponential distribution, whereas the high-end tail follows a power law.

The study of income distribution has a long history. Pareto¹⁴ proposed in 1897 that income distribution obeys a universal power law valid for all times and countries. Subsequent studies have often disputed this conjecture. In 1935, Shirras¹⁵ concluded: “There is indeed no Pareto Law. It is time it should be entirely discarded in studies on distribution”. Mandelbrot¹⁶ proposed a “weak Pareto law” applicable only asymptotically to the high incomes. In such a form, Pareto’s proposal is useless for describing the great majority of the population.

Many other distributions of income were proposed: Levy, log-normal, Champernowne, Gamma, and two other forms by Pareto himself (see a systematic survey in the World Bank research publication¹⁷). Theoretical justifications for these proposals form two schools: socio-economic and statistical. The former appeals to economic, political, and demographic factors to explain the distribution of income (e. g.¹⁸), whereas the latter invokes stochastic processes. Gibrat¹⁹ proposed in 1931 that income is governed by a multiplicative random process, which results in a log-normal distribution (see also²⁰). However, Kalecki²¹ pointed out that the width of this distribution is not stationary, but increases in time. Levy and Solomon²² proposed a cut-off at lower incomes, which stabilizes the distribution to a power law.

Many researchers tried to deduce the Pareto law from a theory of stochastic processes. Gibrat¹⁹ proposed in 1931 that income and wealth are governed by multiplicative random processes, which result in a log-normal distribution. These ideas were later followed, among many others, by Montroll and Shlesinger²⁰. However, already in 1945 Kalecki²¹ pointed out that the log-normal distribution is not stationary, because its width increases in time. Modern econophysicists^{22,33,34} also use various versions of multiplicative random processes in theoretical modeling of wealth and income distributions.

Unfortunately, numerous recent papers on this subject do very little or no comparison at all with real statistical data, much of which is widely available these days on the Inter-

net. In order to fill this gap, we analyzed the data on income distribution in the United States (US) from the Bureau of Census and the Internal Revenue Service (IRS) in Ref.³⁵. We found that the individual income of about 95% of population is described by the exponential law. The exponential law, also known in physics as the Boltzmann-Gibbs distribution, is characteristic for a conserved variable, such as energy. In Ref.³⁶, we argued that, because money (cash) is conserved, the probability distribution of money should be exponential. Wealth can increase or decrease by itself, but money can only be transferred from one agent to another. So, wealth is not conserved, whereas money is. The difference is the same as the difference between unrealized and realized capital gains in stock market.

In Sec. II B, we propose that the distribution of individual income is given by an exponential function. This conjecture is inspired by the results of Ch. I,³⁵, where we argued that the probability distribution of money in a closed system of agents is given by the exponential Boltzmann-Gibbs function. We compare our proposal with the census and tax data for individual income in USA. In Sec. II D we show that the exponential distribution has to be amended for the top 5% of incomes by a power-law function. In Sec. II F, we derive the distribution function of income for families with two earners and compare it with census data. In Sec. II G, we discuss the distribution of wealth. In Sec. II H we critically examine several other alternatives proposed in the literature for the distribution of income and wealth. Speculations on the possible origins of the exponential and power-law distribution of income and conclusions for this chapter are given in Sec. III.

B. Distribution of income for individuals

C. Exponential distribution of income

We denote income by the letter r (for “revenue”). The probability distribution function of income, $P(r)$, (called the probability density in book¹⁷) is defined so that the fraction of individuals with income between r and $r + dr$ is $P(r) dr$. This function is normalized to unity (100%): $\int_0^\infty P(r) dr = 1$. We propose that the probability distribution of individual income is exponential:

$$P_1(r) = \exp(-r/R)/R, \quad (7)$$

where the subscript 1 indicates individuals. Function (7) contains one parameter R , equal to the average income: $\int_0^\infty r P_1(r) dr = R$, and analogous to temperature in the Boltzmann-Gibbs distribution³⁵.

From the Survey of Income and Program Participation (SIPP)²³, we downloaded the variable TPTOINC (total income of a person for a month) for the first “wave” (a four-month period) in 1996. Then we eliminated the entries with zero income, grouped the remaining entries into bins of the size 10/3 k\$, counted the numbers of entries inside each bin, and normalized to the total number of entries. The results are shown as the histogram in Fig. 6, where the horizontal scale

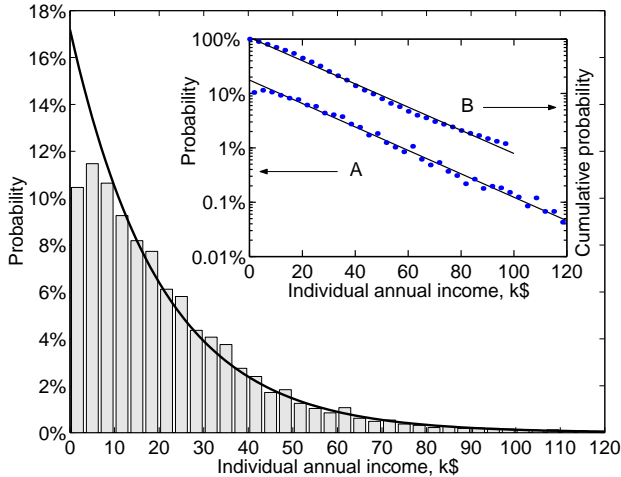


FIG. 6: Histogram: Probability distribution of individual income from the U.S. Census data for 1996²³. Solid line: Fit to the exponential law. Inset plot A: The same with the logarithmic vertical scale. Inset plot B: Cumulative probability distribution of individual income from PSID for 1992²⁴.

has been multiplied by 12 to convert monthly income to an annual figure. The solid line represents a fit to the exponential function (7). In the inset, plot A shows the same data with the logarithmic vertical scale. The data fall onto a straight line, whose slope gives the parameter R in Eq. (7). The exponential law is also often written with the bases 2 and 10: $P_1(r) \propto 2^{-r/R_2} \propto 10^{-r/R_{10}}$. The parameters R , R_2 and R_{10} are given in line (c) of Table I.

	Source	Year	R (\$)	R_2 (\$)	R_{10} (\$)	Set size
a	PSID ²⁴	1992	18,844	13,062	43,390	1.39×10^3
b	IRS ²⁶	1993	19,686	13,645	45,329	1.15×10^8
c	SIPP _p ²³	1996	20,286	14,061	46,710	2.57×10^5
d	SIPP _f ²³	1996	23,242	16,110	53,517	1.64×10^5
e	IRS ²⁵	1997	35,200	24,399	81,051	1.22×10^8

TABLE I: Parameters R , R_2 , and R_{10} obtained by fitting data from different sources to the exponential law (7) with the bases e , 2, and 10, and the sizes of the statistical data sets.

Plot B in the inset of Fig. 6 shows the data from the Panel Study of Income Dynamics (PSID) conducted by the Institute for Social Research of the University of Michigan²⁴. We downloaded the variable V30821 “Total 1992 labor income” for individuals from the Final Release 1993 and processed the data in a similar manner. Shown is the cumulative probability distribution of income $N(r)$ (called the probability distribution in book¹⁷). It is defined as $N(r) = \int_r^\infty P(r') dr'$ and gives the fraction of individuals with income greater than r . For the exponential distribution (7), the cumulative distribution is also exponential: $N_1(r) = \int_r^\infty P_1(r') dr' = \exp(-r/R)$. Thus, R_2 is the median income; 10% of population have income greater than R_{10} and only 1% greater than $2R_{10}$. The points in the inset fall onto a straight line in the

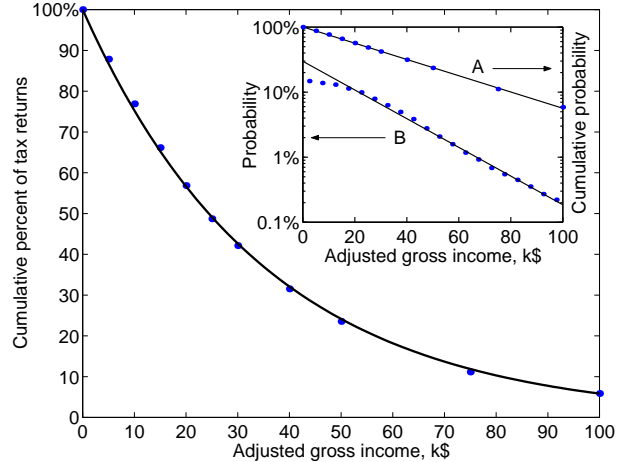


FIG. 7: Points: Cumulative fraction of tax returns vs income from the IRS data for 1997²⁵. Solid line: Fit to the exponential law. Inset plot A: The same with the logarithmic vertical scale. Inset plot B: Probability distribution of individual income from the IRS data for 1993²⁶.

logarithmic scale. The slope is given in line (a) of Table I.

The points in Fig. 7 show the cumulative distribution of tax returns vs income in 1997 from column 1 of Table 1.1 of Ref.²⁵. (We merged 1 k\$ bins into 5 k\$ bins in the interval 1–20 k\$.) The solid line is a fit to the exponential law. Plot A in the inset of Fig. 7 shows the same data with the logarithmic vertical scale. The slope is given in line (e) of Table I. Plot B in the inset of Fig. 7 shows the distribution of individual income from tax returns in 1993²⁶. The logarithmic slope is given in line (b) of Table I.

While Figs. 6 and 7 clearly demonstrate the fit of income distribution to the exponential form, they have the following drawback. Their horizontal axes extend to $+\infty$, so the high-income data are left outside of the plots. The standard way to represent the full range of data is the so-called Lorenz curve (for an introduction to the Lorenz curve and Gini coefficient, see book¹⁷). The horizontal axis of the Lorenz curve, $x(r)$, represents the cumulative fraction of population with income below r , and the vertical axis $y(r)$ represents the fraction of income this population accounts for:

$$x(r) = \int_0^r P(r') dr', \quad y(r) = \frac{\int_0^r r' P(r') dr'}{\int_0^\infty r' P(r') dr'}. \quad (8)$$

As r changes from 0 to ∞ , x and y change from 0 to 1, and Eq. (8) parametrically defines a curve in the (x, y) -space.

Substituting Eq. (7) into Eq. (8), we find

$$x(\tilde{r}) = 1 - \exp(-\tilde{r}), \quad y(\tilde{r}) = x(\tilde{r}) - \tilde{r} \exp(-\tilde{r}), \quad (9)$$

where $\tilde{r} = r/R$. Excluding \tilde{r} , we find the explicit form of the Lorenz curve for the exponential distribution:

$$y = x + (1 - x) \ln(1 - x). \quad (10)$$

R drops out, so Eq. (10) has no fitting parameters.

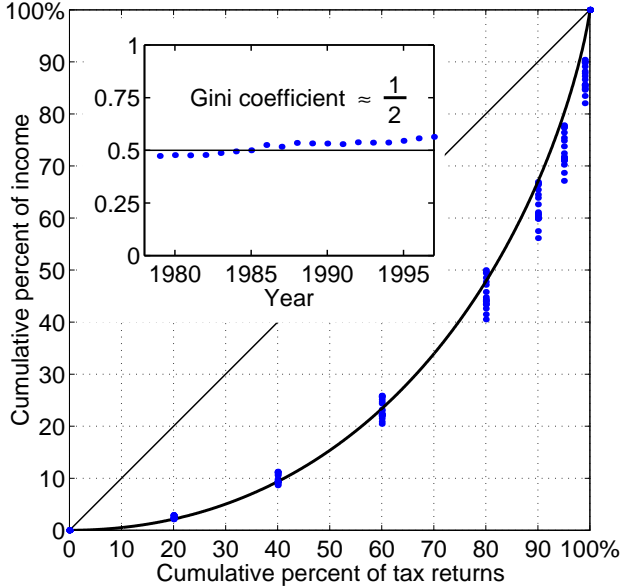


FIG. 8: Solid curve: Lorenz plot for the exponential distribution. Points: IRS data for 1979–1997²⁷. Inset points: Gini coefficient data from IRS²⁷. Inset line: The calculated value 1/2 of the Gini coefficient for the exponential distribution.

The function (10) is shown as the solid curve in Fig. 8. The straight diagonal line represents the Lorenz curve in the case where all population has equal income. Inequality of income distribution is measured by the Gini coefficient G , the ratio of the area between the diagonal and the Lorenz curve to the area of the triangle beneath the diagonal

$$G = 2 \int_0^1 (x - y) dx \quad (11)$$

The Gini coefficient is confined between 0 (no inequality) and 1 (extreme inequality). By substituting Eq. (10) into the integral, we find the Gini coefficient for the exponential distribution: $G_1 = 1/2$.

The points in Fig. 8 represent the tax data during 1979–1997 from Ref.²⁷. With the progress of time, the Lorenz points shifted downward and the Gini coefficient increased from 0.47 to 0.56, which indicates increasing inequality during this period. However, overall the Gini coefficient is close to the value 0.5 calculated for the exponential distribution, as shown in the inset of Fig. 8.

D. Power-law tail and “Bose” condensation

As Fig. 8 shows, the Lorenz curve deviates from the theoretical Lorenz curve implied by the exponential distribution, mostly for the top 20% of tax returns. Moreover, as explained in the previous section, the Lorenz curve for a pure exponential distribution is independent of temperature (the scale of the distribution). Therefore the variations in the Lorenz curves over the period 1979–1997 suggest that the shape of the distribution changes.

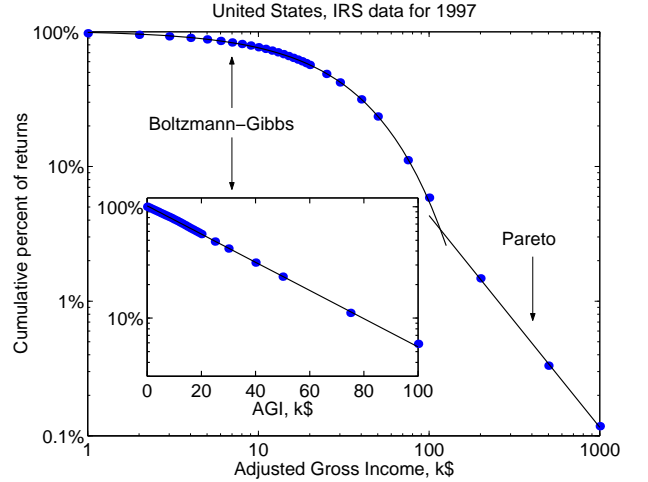


FIG. 9: Cumulative probability distribution of US individual income for 1997 in log-log scale, with points (raw data) and solid lines (exponential and power-law fit). The inset shows the exponential regime and the fit with a Boltzmann–Gibbs distribution in the log-linear scale.

In Sec. II A we mentioned the early proposal of Pareto, who claimed that the income distribution obeys a universal power law valid for all times and countries¹⁴. The Pareto distribution $P(r) = A/r^\alpha$ has several undesirable properties. It diverges for low incomes, and if $\alpha < 2$ the distribution has a diverging first moment. These two properties are never found in real data. Moreover, our study has shown that at least for the overwhelming majority (95%) of the population the distribution of income is exponential.

The data for the remaining top 5% percent of the population is hard to get and often it is unreliable. Because the number of people with income in the top few percents is small, census data is poor. The Internal Revenue Service (IRS) has reliable data but it seldom reports it. We managed to find a data set from IRS which contains high income data²⁵.

Fig. 9 shows United States IRS income data for 1997²⁵. The data points represent the cumulative probability distribution in log-log scale. Although for large income values $r > 120k\$$ we have only three data points, the points align on a straight line in accordance with a Pareto power-law distribution.

From the plot it is evident that there is a discontinuity around $120k\$$ where the exponential and power-law regimes intersect. We conclude that it is not possible to describe the entire income distribution with one single differentiable function. The two regimes of the probability distribution are clearly separated and this may be due to different income dynamics in the two regimes. Among others, the Adjusted Gross Income contains capital gains that is stock-market gains/losses. It is conceivable that for the top 5% of the population, capital gains rather than the labor income account for the majority share of the total income. The capital gains contribution to the Adjusted Growth Income may be responsible for the observed power-law in the tail of the income distribution.

We plot the Lorenz curve for income in Fig. 10. As in Sec.

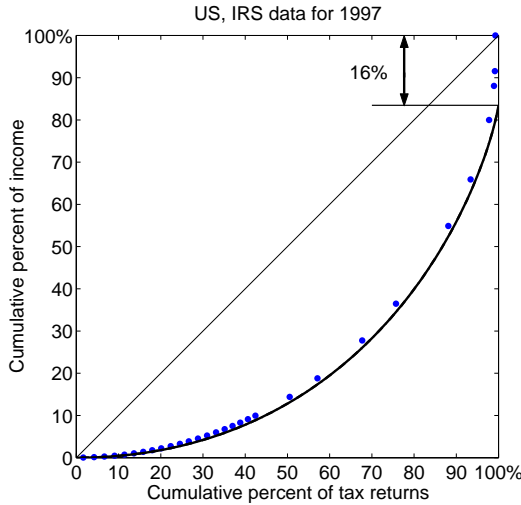


FIG. 10: Lorenz plot with points (raw data) and solid line (function (12) with fraction $b = 16\%$).

II B the horizontal and vertical coordinates are the cumulative population $x(r)$ and the cumulative income $y(r)$ from (8). An imaginary line through the data shows an abrupt change in derivative for the last 2% of the tax returns. This sudden change in derivative around the 98% mark on the horizontal axis of Fig. 10 gives an almost infinite slope for the Lorenz curve. Physically, an infinite slope in the Lorenz function for arguments x just slightly less than one, is equivalent to having a finite amount of total society's income in the hand of a very few individuals. We have coined for this effect the name "Bose condensation of income" because of similarities with the celebrated phase-transition from statistical mechanics.

To understand quantitatively the "Bose condensation" of income, we calculate f the ratio of the total income of the society if all the population is described by the exponential law, to the actual total income of the population. For the USA tax income data for 1997 shown in Fig. 10 this fraction was $f = 0.84$, which means that the "condensate" has $b = 1 - f = 16\%$ of the total income of the population. The analytical formula for the Lorenz curve in this case is

$$y = (1 - b)[x + (1 - x) \ln(1 - x)] + b\delta(1 - x), \quad (12)$$

where the first term represents the contribution of the Boltzmann-Gibbs exponential regime and the second term represents the contribution of the Pareto power-law tail. It is remarkable that as in the case of (10), Eq. 12 does not have any fitting parameters. The condensate fraction b is completely determined by temperature, which in turn is determined from the probability distribution.

The function (12) is plotted as a solid line in Fig. 9. One can see that the data systematically deviate from the exponential law because of the income concentrated in the power-law tail; however, the deviation is not very big. The inequality of the US income distribution was also increasing during that time period³⁵, which implies that the size of the "Bose condensate" has increased in time, too.

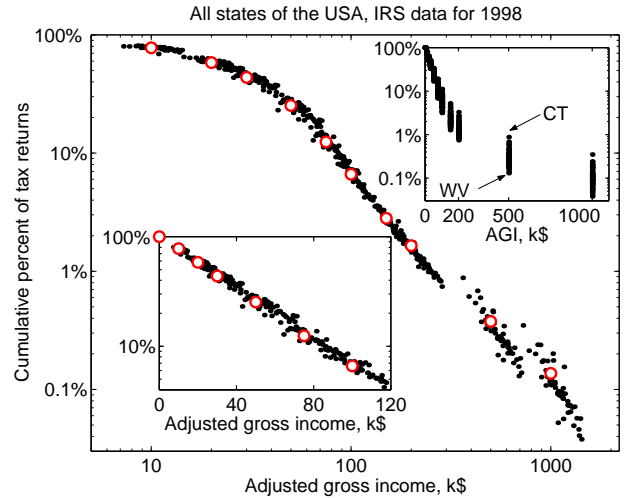


FIG. 11: Cumulative probability distributions of yearly individual income for different states of the USA shown as raw data (top inset) and scaled data in log-log, log-linear (lower inset).

The Gini coefficient defined in (11) can be calculated for the Lorenz curve given by (12). The effect of the power-law tails changes the value of the Gini coefficient from $G_1 = 1/2$ in the case of a pure exponential distribution to $G_b = (1 + b)/2$.

E. Geographical variations in income distribution

In the previous sections we found that the distribution of income is an exponential for the large majority of the population followed by a power-law tail for the top few percent of the population. It would be interesting to establish the universality of this shape for various other countries.

We obtained the data on distribution of the yearly individual income in 1998 for each of the 50 states and the District of Columbia that constitute the USA from the Web site of the IRS⁴². We plot the original raw data for the cumulative distribution of income in log-linear scale in the upper inset of Fig. 11. The points spread significantly, particularly at higher incomes. For example, the fraction of individuals with income greater than 1 M\$ varies by an order of magnitude between different states. However, after we rescale the data in the manner described in the preceding section, the points collapse on a single curve shown in log-log scale in the main panel and log-linear scale in the lower inset. The open circles represent the US average, obtained by treating the combined data for all states as a single set. We observe that the distribution of higher incomes approximately follows a power law with the exponent $\alpha = 1.7 \pm 0.1$, where the ± 0.1 variation includes 70% of all states. On the other hand, for about 95% of individuals with lower incomes, the distribution follows an exponential law with the average US temperature $R_{US} = 36.4$ k\$ ($R_{US}^{(2)} = 25.3$ k\$ and $R_{US}^{(10)} = 83.9$ k\$). The temperatures of the individual states differ from R_{US} by the amounts shown in Table II. For example, the temperature of Connecticut (CT) is 1.25 times higher and the temperature of West Virginia (WV)

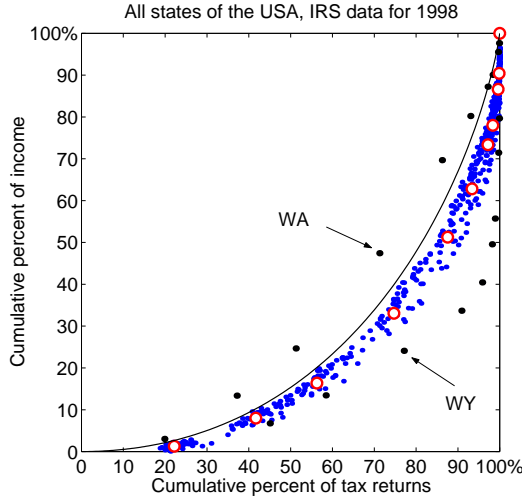


FIG. 12: Lorenz plot with points (raw data) and solid line (function (10) calculated for the exponential law).

TABLE II: Deviations of the state temperatures from the average US temperature.

CT	NJ	MA	MD	VA	CA	NY	IL	CO	NH	AK
25%	24%	14%	14%	9%	9%	7%	6%	6%	5%	5%
DC	DE	MI	WA	MN	GA	TX	RI	AZ	PA	FL
5%	4%	4%	2%	1%	0%	-1%	-3%	-3%	-3%	-4%
KS	OR	HI	NV	NC	WI	IN	UT	MO	VT	TN
-5%	-6%	-7%	-7%	-7%	-8%	-8%	-9%	-9%	-9%	-11%
NE	OH	LA	AL	SC	IA	WY	NM	KY	ID	OK
-12%	-12%	-13%	-13%	-13%	-14%	-14%	-14%	-14%	-15%	-16%
ME	MT	AR	SD	ND	MS	WV				
-16%	-19%	-19%	-20%	-20%	-21%	-22%				

is 0.78 times lower than the average US temperature.

The Lorenz plot for all states is shown in Fig. 12 together with the solid curve representing Eq. (10). The majority of points are well clustered and are not too far from the solid curve. The exceptions are Wyoming (WY) with much higher inequality and the Washington state (WA) with noticeably lower inequality of income distribution. The average US data, shown by open circles, is consistent with our previous results³⁵. Unlike in the UK case, we did not make any adjustment in the US case for individuals with income below the threshold, which appears to be sufficiently low.

We obtained the data on the yearly income distribution in the UK for 1997/8 and 1998/9 from the Web site of the IR³⁹. The data for 1994/5, 1995/6, and 1996/7 were taken from the Annual Abstract of Statistics derived from the IR⁴⁰. The data for these 5 years are presented graphically in Fig. 13. In the upper inset, the original raw data for the cumulative distribution are plotted in log-linear scale. For not too high incomes, the points form straight lines, which implies the exponential distribution $N(r) \propto \exp(-r/R)$, where r stands for income (revenue), and R is the income “temperature”. However, the slopes of these lines are different for different years. The temperatures for the years 1994/5, 1995/6, 1996/7, and 1997/8 differ from the temperature for 1998/9, $R_{UK}^{(98/9)} = 11.7 \text{ k}\mathcal{L}$

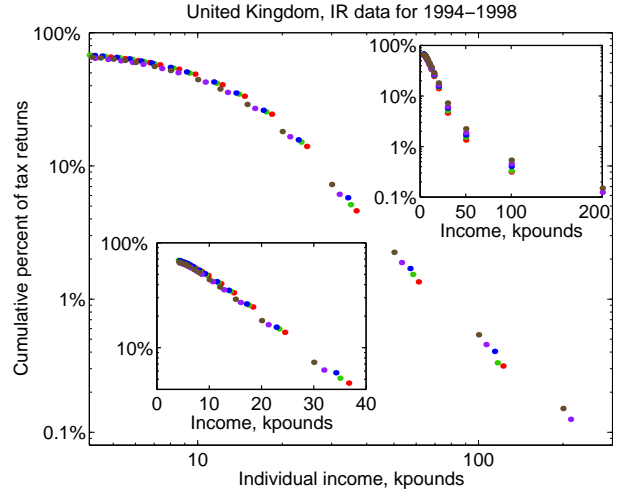


FIG. 13: Cumulative probability distributions of yearly individual income in the UK shown as raw data (top inset) and scaled data in log-log (left panel), log-linear (lower inset), and Lorenz (right panel) coordinates. Solid curve: fit to function (10) calculated for the exponential law.

($R_{UK}^{(2)} = 8.1 \text{ k}\mathcal{L}$ and $R_{UK}^{(10)} = 26.9 \text{ k}\mathcal{L}$), by the factors 0.903, 0.935, 0.954, and 0.943. To compensate for this effect, we rescale the data. We divide the horizontal coordinates (incomes) of the data sets for different years by the quoted above factors and plot the results in log-log scale in the main panel and log-linear scale in the lower inset. We observe scaling: the collapse of points onto a single curve. Thus, the distributions $N_i(r)$ for different years i are described by a single function $f(r/R_i)$. The main panel shows that this scaling function f follows a power law with the exponent $\alpha = 2.0\text{--}2.3$ at high incomes. The lower inset shows that f has an exponential form for about 95% of individuals with lower incomes. These results qualitatively agree with a similar study by Cranshaw⁴¹. He proposed that the $P(r)$ data for lower incomes are better fitted by the Gamma distribution $\Gamma(r) \propto r^\beta \exp(-r/R)$. For simplicity, we chose not to introduce the additional fitting parameter β .

We must mention that the individuals with income below a certain threshold are not required to report to the IR. That is why the data in the lower inset do not extend to zero income. We extrapolate the straight line to zero income and take the intercept with the vertical axis as 100% of individuals. Thus, we imply that the IR data does not account for about 25–27% of individuals with income below the threshold.

The Lorenz curve for the distribution of the UK income is shown in Fig. 14. We treat the number of individuals below the income threshold and their total income as adjustable parameters, which are the horizontal and vertical offsets of the coordinates origin relative to the lowest known data point. These parameters are chosen to fit the Lorenz curve for the exponential law (10) shown as the solid line. The fit is very good, and is illustrated in Fig. 13. The horizontal offsets are 28–34%, which is roughly consistent with the numbers quoted for the lower inset of the left panel.

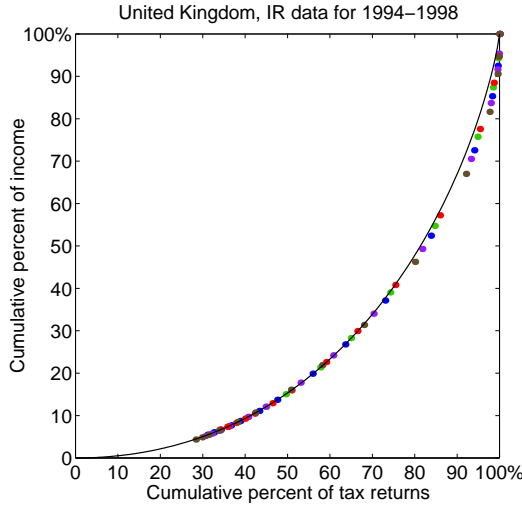


FIG. 14: Cumulative probability distributions of yearly individual income in the UK shown as raw data (top inset) and scaled data in log-log (left panel), log-linear (lower inset), and Lorenz (right panel) coordinates. Solid curve: fit to function (10) calculated for the exponential law.

The income temperature for the UK in 1998/9 was $R_{UK} = 11.7 \text{ k}\mathcal{L}$ and for the US in 1998 was $R_{US} = 36.4 \text{ k\$}$. Using the exchange rate as of December 31, 1998 to convert pounds into dollars⁴⁵, we find that the UK temperature was $R_{UK} = 19.5 \text{ k\$}$, which is 1.87 times lower than the US temperature. The difference in temperatures indicates nonequilibrium, which can be exploited to create a thermal machine³⁶. The gain (profit) produced by such a thermal machine is proportional to the difference in temperatures. In agreement with the second law of thermodynamics, money would flow from a high-temperature system to a low-temperature one. This may explain the huge trade deficit of the USA in global international trade with other, lower-temperature countries. The variation of temperatures between different states of the USA is shown in Table II.

F. Distribution of income for families

Now let us discuss the distribution of income for families with two earners. The family income r is the sum of two individual incomes: $r = r_1 + r_2$. Thus, the probability distribution of the family income is given by the convolution of the individual probability distributions²⁸. If the latter are given by the exponential function (7), the two-earners probability distribution function $P_2(r)$ is

$$P_2(r) = \int_0^r P_1(r') P_1(r - r') dr' = \frac{r}{R^2} e^{-r/R}. \quad (13)$$

The function $P_2(r)$ (13) differs from the function $P_1(r)$ (7) by the prefactor r/R , which reflects the phase space available to compose a given total income out of two individual ones. It is shown as the solid curve in Fig. 15. Unlike $P_1(r)$, which has a

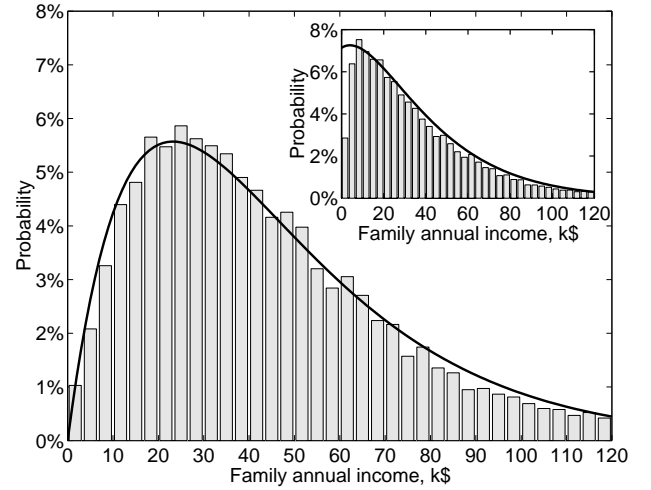


FIG. 15: Histogram: Probability distribution of income for families with two adults in 1996²³. Solid line: Fit to Eq. (13). Inset histogram: Probability distribution of income for all families in 1996²³. Inset solid line: $0.45P_1(r) + 0.55P_2(r)$.

maximum at zero income, $P_2(r)$ has a maximum at $r = R$ and looks qualitatively similar to the family income distribution curves in literature¹⁸.

From the same 1996 SIPP that we used in Sec. II B²³, we downloaded the variable TFTOTINC (the total family income for a month), which we then multiplied by 12 to get annual income. Using the number of family members (the variable EFNP) and the number of children under 18 (the variable RFNKIDS), we selected the families with two adults. Their distribution of family income is shown by the histogram in Fig. 15. The fit to the function (13), shown by the solid line, gives the parameter R listed in line (d) of Table I. The families with two adults and more than two adults constitute 44% and 11% of all families in the studied set of data. The remaining 45% are the families with one adult. Assuming that these two classes of families have two and one earners, we expect the income distribution for all families to be given by the superposition of Eqs. (7) and (13): $0.45P_1(r) + 0.55P_2(r)$. It is shown by the solid line in the inset of Fig. 15 (with R from line (d) of Table I) with the all families data histogram.

By substituting Eq. (13) into Eq. (8), we calculate the Lorenz curve for two-earners families:

$$x(\tilde{r}) = 1 - (1 + \tilde{r})e^{-\tilde{r}}, \quad (14)$$

$$y(\tilde{r}) = x(\tilde{r}) - \tilde{r}^2 e^{-\tilde{r}}/2. \quad (15)$$

It is shown by the solid curve in Fig. 17. Given that $x - y = \tilde{r}^2 \exp(-\tilde{r})/2$ and $dx = \tilde{r} \exp(-\tilde{r}) d\tilde{r}$, the Gini coefficient for two-earners families is: $G_2 = 2 \int_0^1 (x - y) dx = \int_0^\infty \tilde{r}^3 \exp(-2\tilde{r}) d\tilde{r} = 3/8 = 0.375$. The points in Fig. 17 show the Lorenz data and Gini coefficient for family income during 1947–1994 from Table 1 of Ref.²⁹. The Gini coefficient is very close to the calculated value 0.375.

The fundamental assumption which underlies the derivation of (13) is the independence of the two incomes r_1 and r_2 of

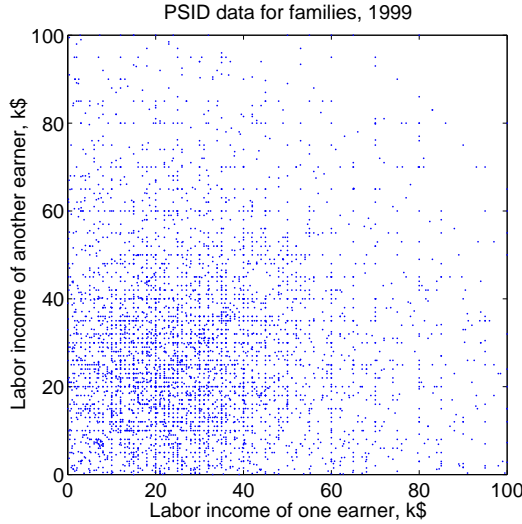


FIG. 16: Points: The income for families with two earners in 1999²⁴. One family is represented by two points (r_1, r_2) and (r_2, r_1) . The existence of correlations between r_1 and r_2 is equivalent to a clustering of points along the diagonal. The data shows little evidence for such correlation.

the two-earner family. While the good fit of the function (13) is an implicit validation of this assumption, it would be good to show that the assumption holds true directly from data. The Census database does not provide the individual values of r_1 and r_2 , but only their sum $r = r_1 + r_2$. We found that the PSID survey²⁴ does have give for a family with two earners, each earners contribution to the total income of the family. We downloaded the variable ER16463 (total labor income, head) and ER16465 (total labor income, wife). We represent in Fig. 16 each family by two points (r_1, r_2) and (r_2, r_1) . The existence of correlations between r_1 and r_2 is equivalent to a clustering of points along the diagonal. Or stated otherwise, the independence of r_1 and r_2 should result in a uniform distribution of points on infinitesimal strips perpendicular to the diagonal. The plotted data shows little, if any evidence for such correlation.

The distributions of the individual and family income differ qualitatively. The former monotonically increases toward the low end and has a maximum at zero income (Fig. 6). The latter, typically being a sum of two individual incomes, has a maximum at a finite income and vanishes at zero (Fig. 15). Thus, the inequality of the family income distribution is smaller. The Lorenz data for families follow the different Eq. (15), again without fitting parameters, and the Gini coefficient is close to the smaller calculated value 0.375 (Fig. 17). Despite different definitions of income by different agencies, the parameters extracted from the fits (Table I) are consistent, except for line (e).

The qualitative difference between the individual and family income distributions was emphasized in Ref.²⁶, which split up joint tax returns of families into individual incomes and combined separately filed tax returns of married couples into family incomes. However, Refs.²⁵ and²⁷ counted only “indi-

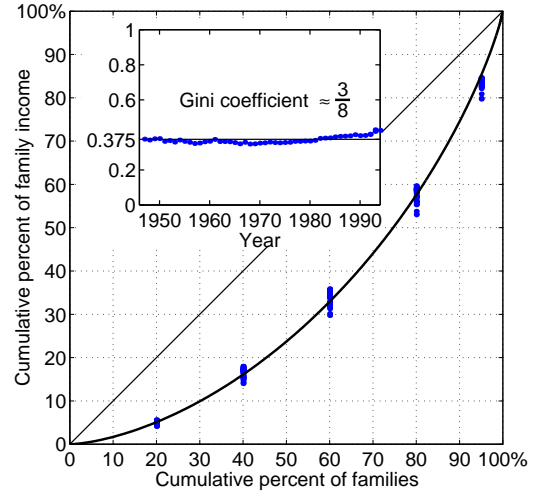


FIG. 17: Solid curve: Lorenz plot (15) for distribution (13). Points: Census data for families, 1947–1994²⁹. Inset points: Gini coefficient data for families from Census²⁹. Inset line: The calculated value $3/8$ of the Gini coefficient for distribution (13).

vidual tax returns”, which also include joint tax returns. Since only a fraction of families file jointly, we assume that the latter contribution is small enough not to distort the tax returns distribution from the individual income distribution significantly. Similarly, the definition of a family for the data shown in the inset of Fig. 15 includes single adults and one-adult families with children, which constitute 35% and 10% of all families. The former category is excluded from the definition of a family for the data²⁹ shown in Fig. 17, but the latter is included. Because the latter contribution is relatively small, we expect the family data in Fig. 17 to approximately represent the two-earners distribution (13). Technically, even for the families with two (or more) adults shown in Fig. 15, we do not know the exact number of earners.

With all these complications, one should not expect perfect accuracy for our fits. There are deviations around zero income in Figs. 6, 7, and 15. The fits could be improved there by multiplying the exponential function by a polynomial. However, the data may not be accurate at the low end because of under-reporting. For example, filing a tax return is not required for incomes below a certain threshold, which ranged in 1999 from \$2,750 to \$14,400³⁰. As the Lorenz curves in Figs. 8 and 17 show, there are also deviations at the high end, possibly where Pareto’s power law is supposed to work. Nevertheless, the exponential law gives an overall good description of income distribution for the great majority of the population.

Figs. 6 and 7 demonstrate that the exponential law (7) fits the individual income distribution very well. The Lorenz data for the individual income follow Eq. (10) without fitting parameters, and the Gini coefficient is close to the calculated value 0.5 (Fig. 8).

It is interesting to study the distribution of the Gini index across the globe. We present in Fig. 18 data from a World Bank publication⁴⁸. This is an question of utmost importance for the World Bank since the distribution of the Gini index

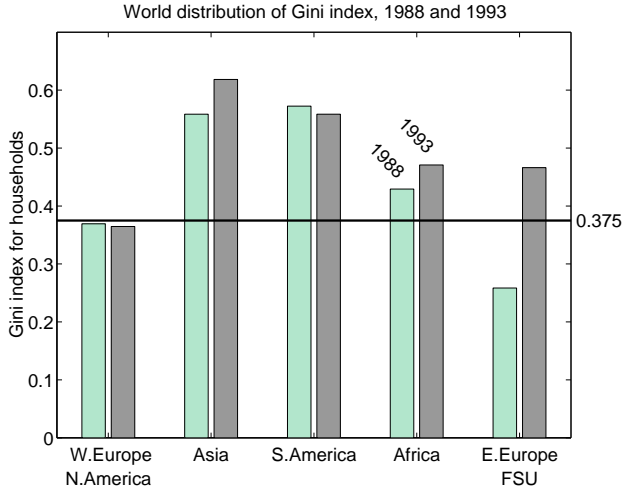


FIG. 18: Distribution of Gini index for households across the globe for two different years, 1988 and 1993⁴⁸. For West Europe and North America, the Gini index is close to 0.375, the value predicted in Sec. II F. A sharp increase in inequality is observed in the Eastern Europe and the Former Soviet Union (FSU) republics after the fall of the “iron curtain” when socialist economies were replaced by market-like economies.

reflects the degree of inequality (poverty) in various regions of the globe. For West Europe and North America, the Gini index is close to 0.375, the value we predicted in Sec. II F. A sharp increase in inequality is observed in the Eastern Europe and the Former Soviet Union (FSU) republics after the fall of the “iron curtain” when socialist economies where replaced by market-like economies. We conjecture that the high value of the Gini index in Asia may be due to the fact that a typical family in Asia has only one earner, so the Gini index is close to a value of 0.5 as observed for individuals.

As the evidence from Fig. 17 and Fig. 18 shows the value of the Gini index varies in time and across the globe, but for the Western world it is close to the value of 0.375, as predicted in Sec. II F.

G. Distribution of wealth

In this section, we discuss the cumulative probability distribution of wealth $N(w)$ =(the number of people whose individual wealth is greater than w)/(the total number of people). A plot of N vs. w is equivalent to a plot of a person’s rank in wealth vs. wealth, which is often used for top richest people³⁷. We will use the power law, $N(w) \propto 1/w^\alpha$, and the exponential law $N(w) \propto \exp(-w/W)$, to fit the data. These distributions are characterized by the exponent α and the “temperature” W . The corresponding probability densities, $P(w) = -dN(w)/dw$, also follow a power law or an exponential law. For the exponential law, it is also useful to define the temperatures $W^{(2)}$ (also known as the median) and $W^{(10)}$ using the bases of 1/2 and 1/10: $N(w) \propto (1/2)^{w/W^{(2)}} \propto (1/10)^{w/W^{(10)}}$.

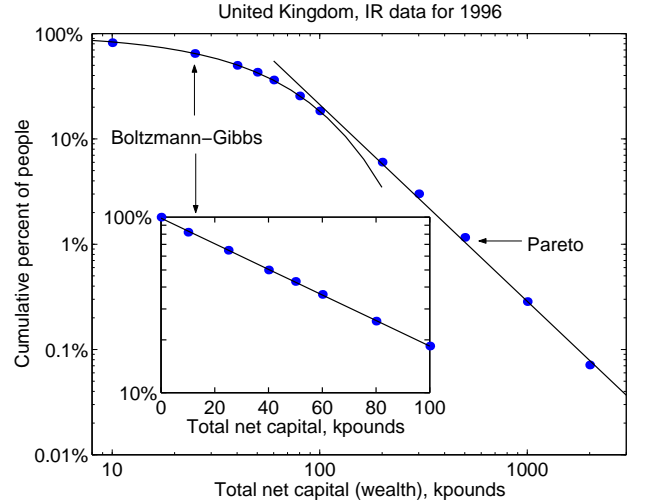


FIG. 19: Left panel: Cumulative probability distribution of total net capital (wealth) shown in log-log, log-linear (inset) coordinates. Points: the actual data. Solid lines: fits to the exponential (Boltzmann-Gibbs) and power (Pareto) laws.

The distribution of wealth is not easy to measure, because people do not report their total wealth routinely. However, when a person dies, all assets must be reported for the purpose of inheritance tax. Using these data and an adjustment procedure, the British tax agency, the Inland Revenue (IR), reconstructed wealth distribution of the whole UK population. In Figs. 19 and 20, we present the 1996 data obtained from their Web site³⁸. Fig. 19 shows the cumulative probability as a function of the personal total net capital (wealth), which is composed of assets (cash, stocks, property, household goods, etc.) and liabilities (mortgages and other debts). The main panel illustrates in the log-log scale that above 100 k£ the data follow a power law with the exponent $\alpha = 1.9$. The inset shows in the log-linear scale that below 100 k£ the data is very well fitted by an exponential distribution with the temperature $W_{UK} = 59.6$ k£ ($W_{UK}^{(2)} = 41.3$ k£ and $W_{UK}^{(10)} = 137.2$ k£).

Since we have established that the distribution of wealth has an exponential regime followed by a power-law tail, we plot the Lorenz curve for wealth in the right panel of Fig. 20. As in Sec. II B the horizontal and vertical coordinates are the cumulative population $x(w)$ and the cumulative wealth $y(w)$:

$$x(w) = \int_0^w P(w') dw', \quad (16)$$

$$y(w) = \int_0^w w' P(w') dw' / \int_0^\infty w' P(w') dw'. \quad (17)$$

As in the case of US income data Fig. 10, there is an abrupt change in the Lorenz curve for the top few percent of people. We interpret this fact in the same way as in Sec. II D, as a “Bose condensation of wealth”. Again, we calculate f the fraction of the total wealth of the society if all people are described by the exponential law, to the actual total wealth of the society. For the United Kingdom in 1996, this frac-

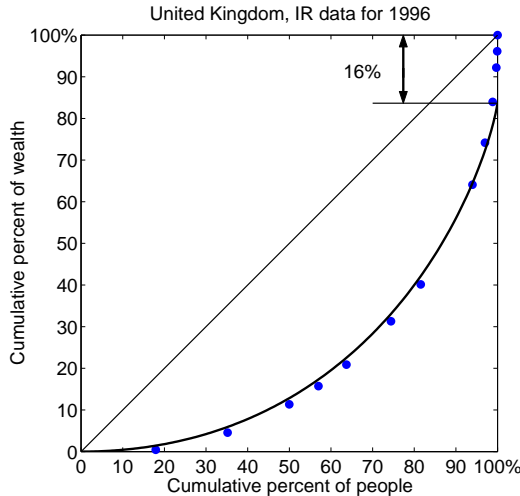


FIG. 20: Points: Lorenz plot for wealth, United Kingdom 1996³⁸. Solid curve: The Lorenz curve given by (18) with a condensate fraction of $b = 16\%$.

tion was $f = 0.84$, which means that the “condensate” has $b = 1 - f = 16\%$ of the total wealth of the system. The functional form for the Lorenz curve for wealth is

$$y = (1 - b)[x + (1 - x)\ln(1 - x)] + b\delta(1 - x). \quad (18)$$

This function is plotted as a solid line in Fig. 20. One can see that the data systematically deviate from the exponential law because of the wealth concentrated in the power-law tail; however, the deviation is not very big. The so-called Gini coefficient^{17,35}, which measures the inequality of wealth distribution, has increased from 64% in 1984 to 68% in 1996³⁸. This value is bigger than the Gini coefficient 50% for a purely exponential distribution³⁵.

While there seems to be no controversy about the fact that a few people hold a finite fraction of the entire wealth, the specific value of this fraction varies widely in the literature. Fractions as high as 80-90% were reported in the literature⁴³ without any support from data. We provide a clear procedure of how to calculate this factor, and we find that $b = 16\%$.

H. Other distributions for income and wealth

As we discussed in the introduction, Sec. II A there have been many proposed functional forms for the distribution of income and wealth. In this section we will investigate several of them.

In Secs. II B, II D, II E and II G we have shown ample evidence to support our findings that the distribution on income and wealth have a similar structure with an exponential part followed by a power-law tail. These results immediately invalidate the proposed Pareto or Gamma distributions as the correct distribution of income.

Another popular distribution which has been proposed for many years as the distribution of income is the lognormal

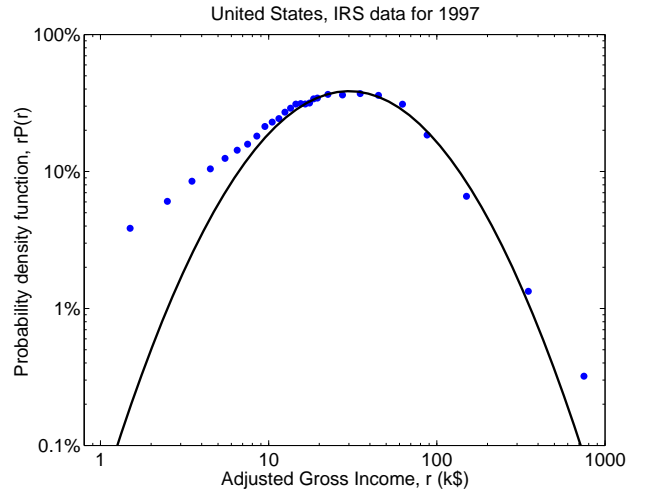


FIG. 21: Points: Calculated probability density $P(r)$ for United States IRS income data for 1997 multiplied by income r , i.e. $rP(r)$. Curve: Fit of data with function $\tilde{P}(r) = rP_{LN}(r)$ (19) with a quadratic function. Clearly, the lognormal distribution fails to describe the data points accurately.

distribution²⁰. The lognormal distribution has the expression

$$P_{LN}(r) = \frac{1}{r\sqrt{2\pi\sigma^2}} \exp\left[-\frac{(\ln r - \mu)^2}{2\sigma^2}\right], \quad (19)$$

where μ and σ are two parameters. As given by (19) the functional form of the lognormal distribution makes it hard to compare it with data. But the function $\tilde{P}(r) = rP_{LN}(r)$ is a quadratic function in a log-log plot. In Fig. 21 we plotted $\ln \tilde{P}(r)$ versus $\ln r$ for the 1997 income data from IRS²⁵. As it can be seen from Fig. 21 a fit of $\tilde{P}(r)$ with a quadratic function cannot be made. The data points show the power-law regime for high incomes. We conclude that the lognormal distribution does not describe the distribution of income.

The distribution of wealth has essentially the same structure as the distribution of income. An exponential regime for low wealth values and a power-law tail for high wealth values. Contrary to the distribution of income, the distribution of wealth appears to have a continuous derivative in the cross-over between the two regimes (see the discussion at the beginning of Sec. II D). The shape of the wealth distribution suggests a modification of the regular exponential Boltzmann-Gibbs distribution for values of wealth $w \gg W$. In the past years, in the context of non-extensive statistical mechanics, Tsallis has proposed a viable alternative to the Boltzmann-Gibbs distribution⁴⁶.

The Tsallis distribution can be obtained by maximizing a generalized entropy and is the subject of a lot of current research. The appeal of the Tsallis distribution is that it has power-law tails for large arguments, and that in certain limit it becomes the exponential distribution. The Tsallis distribution⁴⁶ has the expression

$$P_q(w) = \frac{1}{W_T} \left[1 + (q - 1) \frac{w}{W_T} \right]^{\frac{q}{1-q}}, \quad (20)$$

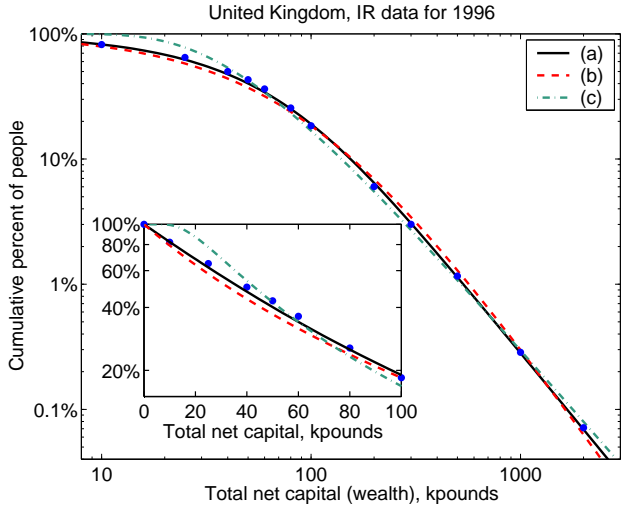


FIG. 22: Points: Internal Revenue wealth data for individuals, 1996³⁸. Curve (a): Fit with the Kaniadakis distribution (21). Curve (b): Fit with the Tsallis distribution (20). Curve (c): Fit with the Bouchaud-Mezard/Solomon-Richmond distribution (22). The inset shows the same three curves in a log-linear scale. The deviations of model (22) from data are evident for small values of income.

where W_T is the dimensional parameter of the Tsallis distribution, analogous to the temperature of the exponential distribution. In the limit $q \rightarrow 1$, the distribution goes to the exponential form $P_{q=1}(w) \propto e^{-w/W_T}$. For $q > 1$, the distribution has a power-law decay $P_q(w) \sim (1/w)^{q/q-1}$ for values $w \gg W$.

In Fig. 22 we present the fit of UK wealth data with the Tsallis distribution. Overall, the quality of the fit is good. The parameters of the Tsallis distribution implied by the fit are: $q = 1.42$, and for the Tsallis temperature $W_T = 41k\mathcal{L}$.

Another distribution proposed by Kaniadakis⁴⁷ in the context of non-extensive statistical mechanics has the form of a deformed exponential

$$P_\kappa(x) = \left(\sqrt{1 + \kappa^2 x^2} - \kappa x \right)^{1/\kappa}, \quad (21)$$

where $x = w/W_\kappa$. For $\kappa \rightarrow 0$, the distribution has the exponential form $P_{\kappa=0}(w) = e^{-w/W_\kappa}$. For large arguments $w \gg W$, the distribution (21) has the power-law behavior $P_\kappa(w) \approx (1/w)^{1/\kappa}$. The fit with the Kaniadakis distribution is even better than that with the Tsallis distribution, as shown in Fig. 22. The parameters of the fit for the Kaniadakis distribution are: $\kappa = 0.33$ and for the Kaniadakis temperature $W_\kappa = 45k\mathcal{L}$.

A distribution for wealth put forward by Bouchaud and Mézard³³, and independently by Solomon and Richmond³², is

$$P_\alpha(x) = \frac{(\alpha-1)^\alpha}{\Gamma(\alpha)} \frac{\exp(-\frac{\alpha-1}{x})}{x^{\alpha+1}}, \quad (22)$$

where $x = w/W_c$. This distribution has an exponentially sharp cut-off for wealths $w \ll W_c$, and a power-law tail $P_\alpha(w) \propto 1/w^{\alpha+1}$ for $w \gg W_c$. The fit of the UK wealth

data with the distribution (22) is presented in Fig. 22. The values we obtain for the parameters are: $\alpha = 1.93$ and $W_c = 74 k\mathcal{L}$. The distribution (22) has its maximum at $x_{max} = (\alpha-1)/(\alpha+1) = 0.32$, which essentially states that for $w > 0.32W_c = 23k\mathcal{L}$ the distribution is a power law. As seen in Fig. 22 this claim is not supported by data. Moreover, the percent of people in the power-law tail predicted by the distribution (22), $\int_{x_{max}}^\infty dx P_\alpha(x) = 81\%$, is clearly much larger than what is observed from the Lorenz curve for wealth, Fig. 20.

All three proposed distributions (20,21,22) seem to capture well the power-law tail. In the inset of Fig. 22 a log-linear scale is used, and this makes the discrepancy between (22) and data much more evident. The distribution (22) is clearly inappropriate for low incomes.

I. Conclusions

Our analysis of the data shows that there are two clear regimes in the distribution of individual income. For low and moderate incomes up to approximately 95% of the total population, the distribution is well described by an exponential, while the income of the top 5% individuals is described by a power-law (Pareto) regime.

The exponential Boltzmann-Gibbs distribution naturally applies to quantities that obey a conservation law, such as energy or money³⁵. However, there is no fundamental reason why the sum of incomes (unlike the sum of money) must be conserved. Indeed, income is a term in the time derivative of one's money balance (the other term is spending). Maybe incomes obey an approximate conservation law, or somehow the distribution of income is simply proportional to the distribution of money, which is exponential³⁵.

Another explanation involves hierarchy. Groups of people have leaders, which have leaders of a higher order, and so on. The number of people decreases geometrically (exponentially) with the hierarchical level. If individual income increases linearly with the hierarchical level, then the income distribution is exponential. However, if income increases multiplicatively, then the distribution follows a power law³¹. For moderate incomes below \$100,000, the linear increase may be more realistic. A similar scenario is the Bernoulli trials²⁸, where individuals have a constant probability of increasing their income by a fixed amount.

We found scaling in the cumulative probability distributions $N(r)$ of individual income r derived from the tax statistics for different years in the UK and for different states in the US. The distributions $N_i(r)$ have the scaling form $f(r/R_i)$, where the scale R_i (the temperature) varies from one data set i to another, but the scaling function f does not. The function f has an exponential (Boltzmann-Gibbs) form at the low end, which covers about 95% of individuals. At the high end, it follows a power (Pareto) law with the exponents about 2.1 for the UK and 1.7 for the US. Wealth distribution in the UK also has a qualitatively similar shape with the exponent about 1.9 and the temperature $W_{UK} = 60 k\mathcal{L}$. Some of the other values of the exponents found in literature are 1.5 proposed by Pareto

himself ($\alpha = 1.5$), 1.36 found by Levy and Solomon³⁷ for the distribution of wealth in the Forbes 400 list, and 2.05 found by Souma⁴⁴ for the high end of income distribution in Japan. The latter study is similar to our work in the sense that it also uses tax statistics and explores the whole range of incomes, not just the high end. Souma⁴⁴ finds that the probability density $P(r)$ at lower incomes follows a log-normal law with a maximum at a nonzero income. This is in contrast to our results, which suggest that the maximum of $P(r)$ is at zero income. The discrepancy may be due to the high threshold for tax reporting in Japan, which distorts the data at the low end. On the other hand, if the data is indeed valid, it may reflect the actual difference between the social structures of the US/UK and Japan.

III. DISTRIBUTION OF STOCK-PRICE FLUCTUATIONS

A. Introduction

Stochastic dynamics of stock prices is commonly described by a geometric (multiplicative) Brownian motion, which gives a log-normal probability distribution for stock price changes (returns)⁵⁰. However, numerous observations show that the tails of the distribution decay slower than the log-normal distribution predicts (the so-called “fat-tails” effect)^{51,52,53}. Particularly, much attention was devoted to the power-law tails^{54,55}. The geometric Brownian motion model has two parameters: the drift μ , which characterizes the average growth rate, and the volatility σ , which characterizes the noisiness of the process. There is empirical evidence and a set of stylized facts indicating that volatility, instead of being a constant parameter, is driven by a mean-reverting stochastic process^{56,57}. Various mathematical models with stochastic volatility have been discussed in literature^{58,59,60,61}.

In this chapter, we study a particular stochastic volatility model, where the square root of the stock-price volatility, called the variance, follows a random process known in financial literature as the Cox-Ingersoll-Ross process and in mathematical statistics as the Feller process^{57,60}. We solve the Fokker-Planck equation for this model exactly and find the joint probability distribution of returns and variance as a function of time, conditional on the initial value of variance. The solution is obtained in two different ways: using the method of characteristics⁶² and the method of path integrals^{63,64,65}. The latter is more familiar to physicists working in finance^{61,66}.

While returns are readily known from a financial time series data, variance is not given directly, so it acts as a hidden stochastic variable. Thus, we integrate the joint probability distribution over variance and obtain the marginal probability distribution of returns *unconditional* on variance. The latter distribution can be directly compared with financial data. We find excellent agreement between our results and the Dow-Jones data for the period of 1982–2001. Using only four fitting parameters, our equations very well reproduce the probability distribution of returns for time lags between 1 and 250 trading days. This is in contrast to popular ARCH, GARCH, EGARCH, TARCH, and similar models, where the number of parameters can easily go to a few dozen⁶⁷.

Our result for the probability distribution of returns has the form of a one-dimensional Fourier integral, which is easily calculated numerically or, in certain asymptotical limits, analytically. For large returns, we find that the probability distribution is exponential in log-returns, which implies a power-law distribution for returns, and we calculate the time dependence of the corresponding exponents. In the limit of long times, the probability distribution exhibits scaling. It becomes a function of a single combination of return and time, with the scaling function expressed in terms of a Bessel function. The Dow-Jones data follow the predicted scaling function for seven orders of magnitude.

The original theory of option pricing was developed by Black and Scholes for the geometric Brownian motion model⁵⁰. Numerous attempts to improve it using stochastic volatility models have been made^{57,58,59,60,61}. Particularly, option pricing for the same model as in our paper⁴⁹ was investigated by Heston⁶⁰. Empirical studies⁶⁸ show that Heston’s theory fares better than the Black-Scholes model, but still does not fully capture the real-market option prices. Since our paper⁴⁹ gives a closed-form time-dependent expression for the probability distribution of returns that agrees with financial data, it can serve as a starting point for a better theory of option pricing.

B. The model

We consider a stock, whose price S_t , as a function of time t , obeys the stochastic differential equation of a geometric (multiplicative) Brownian motion⁵⁰:

$$dS_t = \mu S_t dt + \sigma_t S_t dW_t^{(1)}. \quad (23)$$

Here the subscript t indicates time dependence, μ is the drift parameter, $W_t^{(1)}$ is the standard random Wiener process⁸¹, and σ_t is a time-dependent parameter, called the stock volatility, which characterizes the noisiness of the Wiener process.

Since any solution of (23) depends only on σ_t^2 , it is convenient to introduce the new variable $v_t = \sigma_t^2$, which is called the variance. We assume that v_t obeys the following mean-reverting stochastic differential equation:

$$dv_t = -\gamma(v_t - \theta) dt + \kappa\sqrt{v_t} dW_t^{(2)}. \quad (24)$$

Here θ is the long-time mean of v , γ is the rate of relaxation to this mean, $W_t^{(2)}$ is the standard Wiener process, and κ is a parameter that we call the variance noise. Eq. (24) is known in financial literature as the Cox-Ingersoll-Ross (CIR) process and in mathematical statistics as the Feller process⁵⁷ (p. 42). Alternative equations for v_t , with the last term in (24) replaced by $\kappa dW_t^{(2)}$ or by $\kappa v_t dW_t^{(2)}$, are also discussed in literature⁵⁸. However, in this chapter, we study only the case given by Eq. (24).

We take the Wiener process appearing in (24) to be correlated with the Wiener process in (23):

$$dW_t^{(2)} = \rho dW_t^{(1)} + \sqrt{1 - \rho^2} dZ_t, \quad (25)$$

where Z_t is a Wiener process independent of $W_t^{(1)}$, and $\rho \in [-1, 1]$ is the correlation coefficient. A negative correlation ($\rho < 0$) between $W_t^{(1)}$ and $W_t^{(2)}$ is known as the leverage effect⁵⁷ (p. 41).

It is convenient to change the variable in (23) from price S_t to log-return $r_t = \ln(S_t/S_0)$. Using Itô's formula⁶⁹, we obtain the equation satisfied by r_t :

$$dr_t = \left(\mu - \frac{v_t}{2} \right) dt + \sqrt{v_t} dW_t^{(1)}. \quad (26)$$

The parameter μ can be eliminated from (26) by changing the variable to $x_t = r_t - \mu t$, which measures log-returns relative to the growth rate μ :

$$dx_t = -\frac{v_t}{2} dt + \sqrt{v_t} dW_t^{(1)}. \quad (27)$$

Where it does not cause confusion with r_t , we use the term "log-return" also for the variable x_t .

Equations (27) and (24) define a two-dimensional stochastic process for the variables x_t and v_t . This process is characterized by the transition probability $P_t(x, v | v_i)$ to have log-return x and variance v at time t given the initial log-return $x = 0$ and variance v_i at $t = 0$. Time evolution of $P_t(x, v | v_i)$ is governed by the Fokker-Planck (or forward Kolmogorov) equation⁶⁹

$$\begin{aligned} \frac{\partial}{\partial t} P &= \gamma \frac{\partial}{\partial v} [(v - \theta)P] + \frac{1}{2} \frac{\partial}{\partial x} (vP) \\ &+ \rho \kappa \frac{\partial^2}{\partial x \partial v} (vP) + \frac{1}{2} \frac{\partial^2}{\partial x^2} (vP) + \frac{\kappa^2}{2} \frac{\partial^2}{\partial v^2} (vP). \end{aligned} \quad (28)$$

The initial condition for (28) is a product of two delta functions

$$P_{t=0}(x, v | v_i) = \delta(x) \delta(v - v_i). \quad (29)$$

The variance v is a positive quantity, so Eq. (28) is defined only for $v > 0$. However, when solving (28), it is convenient to extend the domain of v so that $v \in (-\infty, \infty)$. If $2\gamma\theta > \kappa^2$, such an extension does not change the solution of the equation, because, given that $P = 0$ for $v < 0$ at the initial time $t = 0$, the condition $P_t(x, v < 0) = 0$ is preserved for all later times $t > 0$. In order to demonstrate this, let us consider (28) in the limit $v \rightarrow 0$:

$$\frac{\partial}{\partial t} P = - \left(\gamma\theta - \frac{\kappa^2}{2} \right) \frac{\partial P}{\partial v} + \gamma P + \rho \kappa \frac{\partial P}{\partial x}. \quad (30)$$

Eq. (30) is a first-order partial differential equation (PDE), which describes propagation of P from negative v to positive v with the positive velocity $\gamma\theta - \kappa^2/2$. Thus, the nonzero function $P(x, v > 0)$ does not propagate to $v < 0$, and $P_t(x, v < 0)$ remains zero at all times t . Alternatively, it is possible to show⁵⁰ (p. 67) that, if $2\gamma\theta > \kappa^2$, the random process (24) starting in the domain $v > 0$ can never reach the domain $v < 0$.

The probability distribution of the variance itself, $\Pi_t(v) = \int dx P_t(x, v)$, satisfies the equation

$$\frac{\partial}{\partial t} \Pi_t(v) = \frac{\partial}{\partial v} [\gamma(v - \theta)\Pi_t(v)] + \frac{\kappa^2}{2} \frac{\partial^2}{\partial v^2} [v\Pi_t(v)], \quad (31)$$

which is obtained from (28) by integration over x . Eq. (31) has the stationary solution

$$\Pi_*(v) = \frac{\alpha^{\beta+1}}{\Gamma(\beta+1)} v^\beta e^{-\alpha v}, \quad \alpha = \frac{2\gamma}{\kappa^2}, \quad \beta = \alpha\theta - 1, \quad (32)$$

which is the Gamma distribution. The maximum of $\Pi_*(v)$ is reached at $v_{max} = \beta/\alpha = \theta - \kappa^2/2\gamma$. The width w of $\Pi_*(v)$ can be estimated using the curvature at the maximum $w \approx (\kappa^2/2\gamma) \sqrt{2\gamma\theta/\kappa^2 - 1}$. The shape of $\Pi_*(v)$ is characterized by the dimensionless ratio

$$\chi = \frac{v_{max}}{w} = \sqrt{\frac{2\gamma\theta}{\kappa^2} - 1}. \quad (33)$$

When $2\gamma\theta/\kappa^2 \rightarrow \infty$, $\chi \rightarrow \infty$ and $\Pi_*(v) \rightarrow \delta(v - \theta)$.

C. Solution of the Fokker-Planck equation

Since x appears in (28) only in the derivative operator $\partial/\partial x$, it is convenient to make the Fourier transform

$$P_t(x, v | v_i) = \frac{1}{2\pi} \int_{-\infty}^{+\infty} dp_x e^{ip_x x} \bar{P}_{t,p_x}(v | v_i). \quad (34)$$

Inserting (34) into (28), we find

$$\begin{aligned} \frac{\partial}{\partial t} \bar{P} &= \gamma \frac{\partial}{\partial v} [(v - \theta)\bar{P}] \\ &- \left[\frac{p_x^2 - ip_x}{2} v - i\rho\kappa p_x \frac{\partial}{\partial v} v - \frac{\kappa^2}{2} \frac{\partial^2}{\partial v^2} v \right] \bar{P}. \end{aligned} \quad (35)$$

Eq. (35) is simpler than (28), because the number of variables has been reduced to two, v and t , whereas p_x only plays the role of a parameter.

Since Eq. (35) is linear in v and quadratic in $\partial/\partial v$, it can be simplified by taking the Fourier transform over v

$$\bar{P}_{t,p_x}(v | v_i) = \frac{1}{2\pi} \int_{-\infty}^{+\infty} dp_v e^{ip_v v} \tilde{P}_{t,p_x}(p_v | v_i). \quad (36)$$

The PDE satisfied by $\tilde{P}_{t,p_x}(p_v | v_i)$ is of the first order

$$\left[\frac{\partial}{\partial t} + \left(\Gamma p_v + \frac{i\kappa^2}{2} p_v^2 + \frac{ip_x^2 + p_x}{2} \right) \frac{\partial}{\partial p_v} \right] \tilde{P} = -i\gamma\theta p_v \tilde{P}, \quad (37)$$

where we introduced the notation

$$\Gamma = \gamma + i\rho\kappa p_x. \quad (38)$$

Eq. (37) has to be solved with the initial condition

$$\tilde{P}_{t=0,p_x}(p_v | v_i) = \exp(-ip_v v_i). \quad (39)$$

The solution of the PDE (37) is given by the method of characteristics⁶²:

$$\tilde{P}_{t,p_x}(p_v | v_i) = \exp \left(-i\tilde{p}_v(0)v_i - i\gamma\theta \int_0^t d\tau \tilde{p}_v(\tau) \right), \quad (40)$$

where the function $\tilde{p}_v(\tau)$ is the solution of the characteristic (ordinary) differential equation

$$\frac{d\tilde{p}_v(\tau)}{d\tau} = \Gamma\tilde{p}_v(\tau) + \frac{i\kappa^2}{2}\tilde{p}_v^2(\tau) + \frac{i}{2}(p_x^2 - ip_x) \quad (41)$$

with the boundary condition $\tilde{p}_v(t) = p_v$ specified at $\tau = t$. The solution (40) can be also obtained using the method of path integrals described in Sec. III D. The differential equation (41) is of the Riccati type with constant coefficients⁷⁰, and its solution is

$$\tilde{p}_v(\tau) = -i\frac{2\Omega}{k^2}\frac{1}{\zeta e^{\Omega(\tau-t)} - 1} + i\frac{\Gamma - \Omega}{k^2}, \quad (42)$$

where we introduced the frequency

$$\Omega = \sqrt{\Gamma^2 + \kappa^2(p_x^2 - ip_x)}. \quad (43)$$

and the coefficient

$$\zeta = 1 - i\frac{2\Omega}{\kappa^2 p_v - i(\Gamma - \Omega)}. \quad (44)$$

Substituting (42) into (40) and taking the Fourier transforms (34) and (36), we get the solution

$$P_t(x, v | v_i) = \frac{1}{(2\pi)^2} \int_{-\infty}^{+\infty} dp_x dp_v e^{ip_x x + ip_v v} \times \exp \left\{ -ip_v(0)v_i + \frac{\gamma\theta(\Gamma - \Omega)t}{\kappa^2} - \frac{2\gamma\theta}{\kappa^2} \ln \frac{\zeta - e^{-\Omega t}}{\zeta - 1} \right\} \quad (45)$$

of the original Fokker-Planck equation (28) with the initial condition (29), where $\tilde{p}_v(\tau = 0)$ is given by (42).

D. Path-Integral Solution

The Fokker-Planck equation (35) can be thought of as a Schrödinger equation in imaginary (Euclidean) time:

$$\frac{\partial}{\partial t} \overline{P}_{t,p_x}(v | v_i) = -\hat{H}_{p_x}(\hat{p}_v, \hat{v}) \overline{P}_{t,p_x}(v | v_i) \quad (46)$$

with the Hamiltonian

$$\hat{H} = \frac{\kappa^2}{2}\hat{p}_v^2\hat{v} - i\gamma\hat{p}_v(\hat{v} - \theta) + \frac{p_x^2 - ip_x}{2}\hat{v} + \rho\kappa p_x\hat{p}_v\hat{v}. \quad (47)$$

In (47) we treat \hat{p}_v and \hat{v} as canonically conjugated operators with the commutation relation $[\hat{v}, \hat{p}_v] = i$. The transition probability $\overline{P}_{p_x}(v, t | v_i)$ is the matrix element of the evolution operator $\exp(-\hat{H}t)$ and has a path-integral representation^{63,64,65}

$$\overline{P}_{t,p_x}(v | v_i) = \langle v | e^{-\hat{H}t} | v_i \rangle = \int \mathcal{D}v \mathcal{D}p_v e^{S_{p_x}[p_v(\tau), v(\tau)]}. \quad (48)$$

Here the action functional $S_{p_x}[p_v(\tau), v(\tau)]$ is

$$S_{p_x} = \int_0^t d\tau \{ ip_v(\tau)\dot{v}(\tau) - H_{p_x}[p_v(\tau), v(\tau)] \}, \quad (49)$$

and the dot denotes the time derivative. The phase-space path integral (48) is the sum over all possible paths $p_v(\tau)$ and $v(\tau)$ with the boundary conditions $v(\tau = 0) = v_i$ and $v(\tau = t) = v$ imposed on v .

It is convenient to integrate the first term on the r.h.s. of (49) by parts:

$$S_{p_x} = i[p_v(t)v - \tilde{p}_v(0)v_i] - i\gamma\theta \int_0^t d\tau p_v(\tau) - \int_0^t d\tau \left[ip_v(\tau) + \frac{\delta H}{\delta v(\tau)} \right] v(\tau), \quad (50)$$

where we also separated the terms linear in $v(\tau)$ from the Hamiltonian (47). Because $v(\tau)$ enters linearly in the action (50), taking the path integral over $\mathcal{D}v$ generates the delta-functional $\delta[p_v(\tau) - \tilde{p}_v(\tau)]$, where $\tilde{p}_v(\tau)$ is the solution of the ordinary differential equation (41) with a boundary condition specified at $\tau = t$. Taking the path integral over $\mathcal{D}p_v$ resolves the delta-functional, and we find

$$\overline{P}_{t,p_x}(v | v_i) = \int_{-\infty}^{+\infty} \frac{dp_v}{2\pi} e^{i[p_v v - \tilde{p}_v(0)v_i] - i\gamma\theta \int_0^t d\tau \tilde{p}_v(\tau)}, \quad (51)$$

where $\tilde{p}_v(\tau = t) = p_v$. Eq. (51) coincides with (40) after the Fourier transform (36).

E. Averaging over variance

Normally we are interested only in log-returns x and do not care about variance v . Moreover, whereas log-returns are directly known from financial data, variance is a hidden stochastic variable that has to be estimated. Inevitably, such an estimation is done with some degree of uncertainty, which precludes a clear-cut direct comparison between $P_t(x, v | v_i)$ and financial data. Thus, we introduce the probability distribution

$$P_t(x | v_i) = \int_{-\infty}^{+\infty} dv P_t(x, v | v_i), \quad (52)$$

where the hidden variable v is integrated out. The integration of (45) over v generates the delta-function $\delta(p_v)$, which effectively sets $p_v = 0$. Substituting the coefficient ζ from (44) with $p_v = 0$ into (45), we find

$$P_t(x | v_i) = \frac{1}{2\pi} \int_{-\infty}^{+\infty} dp_x e^{ip_x x - v_i \frac{p_x^2 - ip_x}{\Gamma + \Omega \coth(\Omega t/2)}} \times e^{-\frac{2\gamma\theta}{\kappa^2} \ln(\cosh \frac{\Omega t}{2} + \frac{\gamma}{\Omega} \sinh \frac{\Omega t}{2}) + \frac{\gamma\Gamma\theta t}{\kappa^2}}. \quad (53)$$

To check the validity of (53), let us consider the case $\kappa = 0$. In this case, the stochastic term in (24) is absent, so the time evolution of variance is deterministic:

$$v(t) = \theta + (v_i - \theta)e^{-\gamma t}. \quad (54)$$

Then process (27) gives a Gaussian distribution for x ,

$$P_t^{(\kappa=0)}(x | v_i) = \frac{1}{\sqrt{2\pi t \bar{v}_t}} \exp \left(-\frac{(x + \bar{v}_t t/2)^2}{2\bar{v}_t t} \right), \quad (55)$$

with the time-averaged variance $\bar{v}_t = \frac{1}{t} \int_0^t d\tau v(\tau)$. Eq. (55) demonstrates that the probability distribution of stock price S is log-normal in the case $\kappa = 0$. On the other hand, by taking the limit $\kappa \rightarrow 0$ and integrating over p_x in (53), we reproduce the same expression (55).

Eq. (53) cannot be directly compared with financial time series data, because it depends on the unknown initial variance v_i . In order to resolve this problem, we assume that v_i has the stationary probability distribution $\Pi_*(v_i)$, which is given by (32).⁸² Thus we introduce the probability distribution $P_t(x)$ by averaging (53) over v_i with the weight $\Pi_*(v_i)$:

$$P_t(x) = \int_0^\infty dv_i \Pi_*(v_i) P_t(x | v_i). \quad (56)$$

The integral over v_i is similar to the one of the Gamma function and can be taken explicitly. The final result is the Fourier integral

$$P_t(x) = \frac{1}{2\pi} \int_{-\infty}^{+\infty} dp_x e^{ip_x x + F_t(p_x)} \quad (57)$$

with

$$\begin{aligned} F_t(p_x) &= \frac{\gamma\Gamma\theta t}{\kappa^2} \\ &- \frac{2\gamma\theta}{\kappa^2} \ln \left[\cosh \frac{\Omega t}{2} + \frac{\Omega^2 - \Gamma^2 + 2\gamma\Gamma}{2\gamma\Omega} \sinh \frac{\Omega t}{2} \right]. \end{aligned} \quad (58)$$

The variable p_x enters (58) via the variables Γ from (38) and Ω from (43). It is easy to check that $P_t(x)$ is real, because $\text{Re}F$ is an even function of p_x and $\text{Im}F$ is an odd one. One can also check that $F_t(p_x = 0) = 0$, which implies that $P_t(x)$ is correctly normalized at all times: $\int dx P_t(x) = 1$. The second term in the r.h.s. of (58) vanishes when $\rho = 0$, i.e. when there are no correlations between stock price and variance. The simplified result for the case $\rho = 0$ is given in III F by Eqs. (72), (73), and (74).

Eqs. (57) and (58) for the probability distribution $P_t(x)$ of log-return x at time t are the central analytical result of the chapter. The integral in (57) can be calculated numerically or, in certain regimes discussed in Secs. III F and III G, analytically. In Fig. 23, the calculated function $P_t(x)$, shown by solid lines, is compared with the Dow-Jones data, shown by dots. (Technical details of the data analysis are discussed in Sec. III H.) Fig. 23 demonstrates that, with a fixed set of the parameters γ , θ , κ , μ , and ρ , Eqs. (57) and (58) very well reproduce the distribution of log-returns x of the Dow-Jones index for all times t . In the log-linear scale of Fig. 23, the tails of $\ln P_t(x)$ vs. x are straight lines, which means that the tails of $P_t(x)$ are exponential in x . For short times, the distribution is narrow, and the slopes of the tails are nearly vertical. As time progresses, the distribution broadens and flattens.

F. Asymptotic behavior for long time t

Eq. (24) implies that variance reverts to the equilibrium value θ within the characteristic relaxation time $1/\gamma$. In this

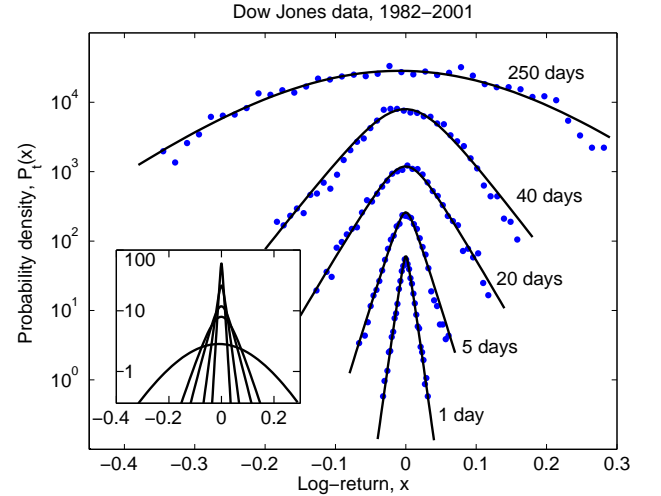


FIG. 23: Probability distribution $P_t(x)$ of log-return x for different time lags t . Points: The Dow-Jones data for $t = 1, 5, 20, 40$, and 250 trading days. Solid lines: Fit of the data with Eqs. (57) and (58). For clarity, the data points and the curves for successive t are shifted up by the factor of 10 each. The inset shows the curves without vertical shift.

section, we consider the asymptotic limit where time t is much longer than the relaxation time: $\gamma t \gg 2$. According to (38) and (43), this condition also implies that $\Omega t \gg 2$. Then Eq. (58) reduces to

$$F_t(p_x) \approx \frac{\gamma\theta t}{\kappa^2} (\Gamma - \Omega). \quad (59)$$

Let us change of the variable of integration in (57) to

$$p_x = \frac{\omega_0}{\kappa\sqrt{1-\rho^2}} \tilde{p}_x + ip_0, \quad (60)$$

where

$$p_0 = \frac{\kappa - 2\rho\gamma}{2\kappa(1-\rho^2)}, \quad \omega_0 = \sqrt{\gamma^2 + \kappa^2(1-\rho^2)p_0^2}. \quad (61)$$

Substituting (60) into (38), (43), and (59), we transform (57) to the following form

$$P_t(x) = \frac{\omega_0 e^{-p_0 x + \Lambda t}}{\pi\kappa\sqrt{1-\rho^2}} \int_0^\infty d\tilde{p}_x \cos(A\tilde{p}_x) e^{-B\sqrt{1+\tilde{p}_x^2}}, \quad (62)$$

where

$$A = \frac{\omega_0}{\kappa\sqrt{1-\rho^2}} \left(x + \rho \frac{\gamma\theta t}{\kappa} \right), \quad B = \frac{\gamma\theta\omega_0 t}{\kappa^2}, \quad (63)$$

and

$$\Lambda = \frac{\gamma\theta}{2\kappa^2} \frac{2\gamma - \rho\kappa}{1-\rho^2}. \quad (64)$$

According to⁷², the integral in (62) is equal to $B K_1(\sqrt{A^2 + B^2}) / \sqrt{A^2 + B^2}$, where K_1 is the first-order modified Bessel function.

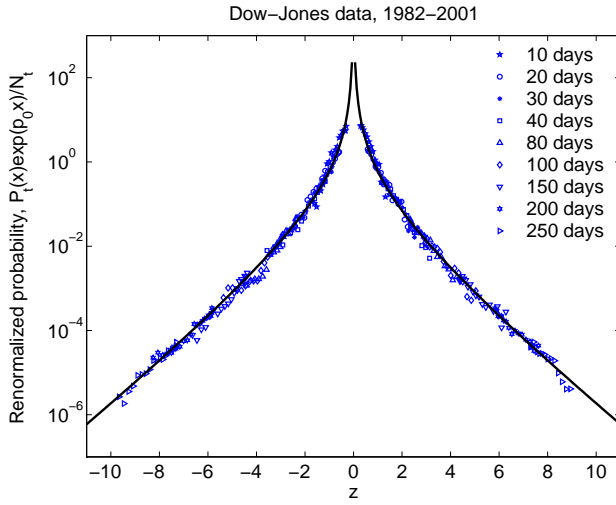


FIG. 24: Renormalized probability density $P_t(x)\exp(p_0x)/N_t$ plotted as a function of the scaling argument z given by (66). Solid line: The scaling function $P_*(z) = K_1(z)/z$ from (65), where K_1 is the first-order modified Bessel function. Symbols: The Dow-Jones data for different time lags t .

Thus, Eq. (57) in the limit $\gamma t \gg 2$ can be represented in the scaling form

$$P_t(x) = N_t e^{-p_0 x} P_*(z), \quad P_*(z) = K_1(z)/z, \quad (65)$$

where the argument $z = \sqrt{A^2 + B^2}$ is

$$z = \frac{\omega_0}{\kappa} \sqrt{\frac{(x + \rho\gamma\theta t/\kappa)^2}{1 - \rho^2} + \left(\frac{\gamma\theta t}{\kappa}\right)^2}, \quad (66)$$

and the time-dependent normalization factor N_t is

$$N_t = \frac{\omega_0^2 \gamma \theta t}{\pi \kappa^3 \sqrt{1 - \rho^2}} e^{\Lambda t}, \quad (67)$$

Eq. (65) demonstrates that, up to the factors N_t and $e^{-p_0 x}$, the dependence of $P_t(x)$ on the two arguments x and t is given by the function $P_*(z)$ of the single scaling argument z in (66). Thus, when plotted as a function of z , the data for different x and t should collapse on the single universal curve $P_*(z)$. This is beautifully illustrated by Fig. 24, where the Dow-Jones data for different time lags t follows the curve $P_*(z)$ for seven decades.

In the limit $z \gg 1$, we can use the asymptotic expression⁷² $K_1(z) \approx e^{-z} \sqrt{\pi/2z}$ in (65) and take the logarithm of P . Keeping only the leading term proportional to z and omitting the subleading term proportional to $\ln z$, we find

$$\ln \frac{P_t(x)}{N_t} \approx -p_0 x - z \quad \text{for } z \gg 1. \quad (68)$$

Let us examine Eq. (68) for large and small $|x|$.

In the first case $|x| \gg \gamma\theta t/\kappa$, Eq. (66) gives $z \approx \omega_0|x|/\kappa\sqrt{1 - \rho^2}$, so Eq. (68) becomes

$$\ln \frac{P_t(x)}{N_t} \approx -p_0 x - \frac{\omega_0}{\kappa\sqrt{1 - \rho^2}} |x|. \quad (69)$$

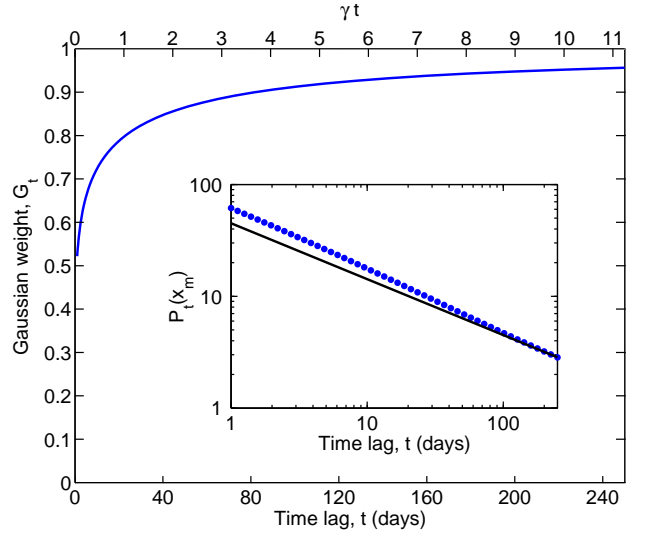


FIG. 25: The fraction G_t of the total probability contained in the Gaussian part of $P_t(x)$ vs. time lag t . Inset: Time dependence of the probability density at maximum $P_t(x_m)$ (points), compared with the Gaussian $t^{-1/2}$ behavior (solid line).

Thus, the probability distribution $P_t(x)$ has the exponential tails (69) for large log-returns $|x|$. Notice that, in the considered limit $\gamma t \gg 2$, the slopes $d \ln P_t(x)/dx$ of the exponential tails (69) do not depend on time t . Because of p_0 , the slopes (69) for positive and negative x are not equal, thus the distribution $P_t(x)$ is not symmetric with respect to up and down price changes. According to (61), this asymmetry is enhanced by a negative correlation $\rho < 0$ between stock price and variance.

In the second case $|x| \ll \gamma\theta t/\kappa$, by Taylor-expanding z in (66) near its minimum and substituting the result into (68), we get

$$\ln \frac{P_t(x)}{N'_t} \approx -p_0 x - \frac{\omega_0(x + \rho\gamma\theta t/\kappa)^2}{2(1 - \rho^2)\gamma\theta t}, \quad (70)$$

where $N'_t = N_t \exp(-\omega_0\gamma\theta t/\kappa^2)$. Thus, for small log-returns $|x|$, the probability distribution $P_t(x)$ is Gaussian with the width increasing linearly in time. The maximum of $P_t(x)$ in (70) is achieved at

$$x_m(t) = -\frac{\gamma\theta t}{2\omega_0} \left(1 + 2 \frac{\rho(\omega_0 - \gamma)}{\kappa}\right). \quad (71)$$

Eq. (71) gives the most probable log-return $x_m(t)$ at time t , and the coefficient in front of t constitutes a correction to the average growth rate μ , so that the actual growth rate is $\bar{\mu} = \mu + dx_m/dt$.

As Fig. 23 illustrates, $\ln P_t(x)$ is indeed linear in x for large $|x|$ and quadratic for small $|x|$, in agreement with (69) and (70). As time progresses, the distribution, which has the scaling form (65) and (66), broadens. Thus, the fraction G_t of the total probability contained in the parabolic (Gaussian) portion of the curve increases, as illustrated in Fig. 25.

In the remainder of the section, we explain the way the Gaussian weight of the distribution has been calculated. As

explained in Sec. III H, the case relevant for comparison with the data is $\rho = 0$. In this case, by shifting the contour of integration in (57) as follows $p_x \rightarrow p_x + i/2$, we find

$$P_t(x) = e^{-x/2} \int_{-\infty}^{+\infty} \frac{dp_x}{2\pi} e^{ip_x x + F_t(p_x)}, \quad (72)$$

where

$$F_t(p_x) = \frac{\gamma^2 \theta t}{\kappa^2} - \frac{2\gamma\theta}{\kappa^2} \ln \left[\cosh \frac{\Omega t}{2} + \frac{\Omega^2 + \gamma^2}{2\gamma\Omega} \sinh \frac{\Omega t}{2} \right] \quad (73)$$

and

$$\Omega = \sqrt{\gamma^2 + \kappa^2(p_x^2 + 1/4)}. \quad (74)$$

Now the function $F_t(p_x)$ is real and symmetric: $F_t(p_x) = F_t(-p_x)$. Thus, the integral in (72) is a symmetric function of x . So it is clear that the only source of asymmetry of $P_t(x)$ in x is the exponential prefactor in (72), as discussed at the end of Sec. III H. Eqs. (72), (73), and (74) are much simpler than those for $\rho \neq 0$.

Let us expand the integral in (72) for small x :

$$P_t(x) \approx e^{-x/2} \left(\mu_0 - \frac{1}{2} \mu_2 x^2 \right), \quad (75)$$

where the coefficients are the first and the second moments of $\exp[F_t(p_x)]$

$$\mu_0(t) = \int_{-\infty}^{+\infty} \frac{dp_x}{2\pi} e^{F_t(p_x)}, \quad \mu_2(t) = \int_{-\infty}^{+\infty} \frac{dp_x}{2\pi} p_x^2 e^{F_t(p_x)}. \quad (76)$$

On the other hand, we know that $P_t(x)$ is Gaussian for small x . So we can write

$$P_t(x) \approx \mu_0 e^{-x/2} e^{-\mu_2 x^2 / 2\mu_0}, \quad (77)$$

with the same coefficients as in (75). If we ignore the existence of fat tails and extrapolate (77) to $x \in (-\infty, \infty)$, the total probability contained in such a Gaussian extrapolation will be

$$G_t = \int_{-\infty}^{+\infty} dx \mu_0 e^{-x/2 - \mu_2 x^2 / 2\mu_0} = \sqrt{\frac{2\pi\mu_0^3}{\mu_2}} e^{\mu_0 / 8\mu_2}. \quad (78)$$

Obviously, $G_t < 1$, because the integral (78) does not take into account the probability contained in the fat tails. Thus, the difference $1 - G_t$ can be taken as a measure of how much the actual distribution $P_t(x)$ deviates from a Gaussian function.

We calculate the moments (76) numerically for the function F given by (73), then determine the Gaussian weight G_t from (78) and plot it in Fig. 25 as a function of time. For $t \rightarrow \infty$, $G_t \rightarrow 1$, i.e. $P_t(x)$ becomes Gaussian for very long time lags, which is known in literature⁵⁵. In the opposite limit $t \rightarrow 0$, $F_t(p_x)$ becomes a very broad function of p_x , so we cannot calculate the moments μ_0 and μ_2 numerically. The singular limit $t \rightarrow 0$ requires an analytical study.

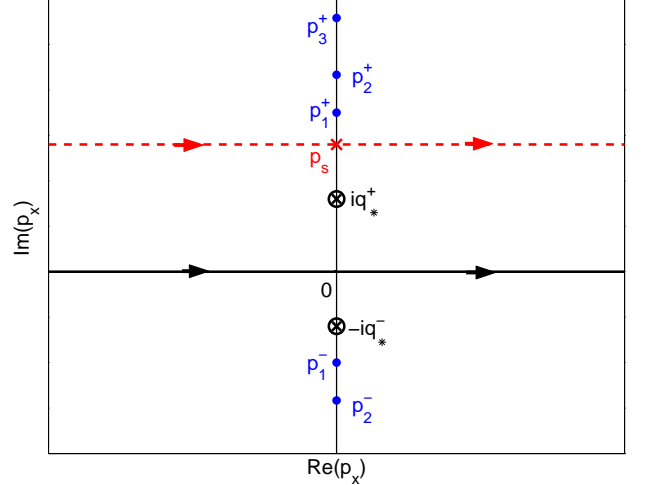


FIG. 26: Complex plane of p_x . Dots: The singularities of $F_t(p_x)$. Circled crosses: The accumulation points $\pm iq_*^\pm$ of the singularities in the limit $\gamma t \gg 2$. Symbol \times : Saddle point p_s , which is located in the upper half-plane for $x > 0$. Dashed line: The contour of integration displaced from the real axis in order to pass through the saddle point p_s .

Fig. 25 shows that, at sufficiently long times, the total probability contained in the non-Gaussian tails becomes negligible, which is known in literature⁵⁵. The inset in Fig. 25 illustrates that the time dependence of the probability density at maximum, $P_t(x_m)$, is close to $t^{-1/2}$, which is characteristic of a Gaussian evolution.

G. Asymptotic behavior for large log-return x

In the complex plane of p_x , function $F(p_x)$ becomes singular at the points p_x where the argument of any logarithm in (58) vanishes. These points are located on the imaginary axis of p_x and are shown by dots in Fig. 26. The singularity closest to the real axis is located on the positive (negative) imaginary axis at the point p_1^+ (p_1^-). At these two points, the argument of the last logarithm in (58) vanishes, and we can approximate $F(p_x)$ by the dominant, singular term: $F(p_x) \approx -(2\gamma\theta/\kappa^2) \ln(p_x - p_1^\pm)$.

For large $|x|$, the integrand of (57) oscillates very fast as a function of p_x . Thus, we can evaluate the integral using the method of stationary phase⁷⁰ by shifting the contour of integration so that it passes through a saddle point of the argument $ip_x x + F(p_x)$ of the exponent in (57). The saddle point position p_s , shown in Fig. 26 by the symbol \times , is determined by the equation

$$ix = - \left. \frac{dF(p_x)}{dp_x} \right|_{p_x=p_s} \approx \frac{2\gamma\theta}{\kappa^2} \times \begin{cases} \frac{1}{p_s - p_1^+}, & x > 0, \\ \frac{1}{p_s - p_1^-}, & x < 0. \end{cases} \quad (79)$$

For a large $|x|$ such that $|xp_1^\pm| \gg 2\gamma\theta/\kappa^2$, the saddle point p_s is very close to the singularity point: $p_s \approx p_1^+$ for $x > 0$ and

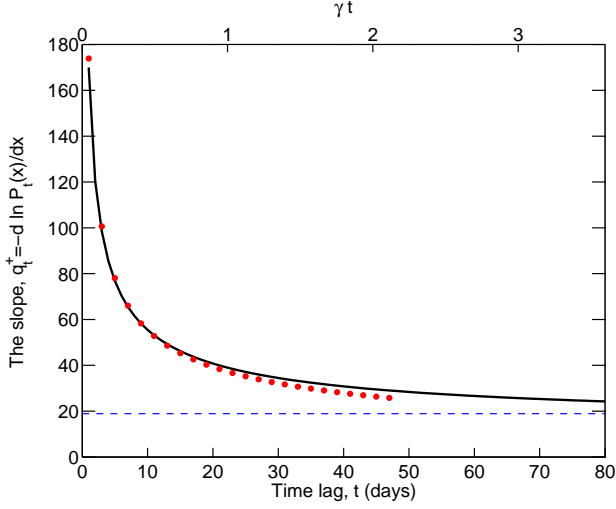


FIG. 27: small Solid line: The slope $q_t^+ = -d \ln P/dx$ of the exponential tail for $x > 0$ as a function of time. Points: The asymptotic approximation (82) for the slope in the limit $\gamma t \ll 2$. Dashed line: The saturation value q_*^+ for $\gamma t \gg 2$, Eq. (81).

$p_s \approx p_1^-$ for $x < 0$. Then the asymptotic expression for the probability distribution is

$$P_t(x) \sim \begin{cases} e^{-xq_t^+}, & x > 0, \\ e^{xq_t^-}, & x < 0, \end{cases} \quad (80)$$

where $q_t^\pm = \mp ip_1^\pm(t)$ are real and positive. Eq. (80) shows that, for all times t , the tails of the probability distribution $P_t(x)$ for large $|x|$ are exponential. The slopes of the exponential tails, $q^\pm = \mp d \ln P/dx$, are determined by the positions p_1^\pm of the singularities closest to the real axis.

These positions $p_1^\pm(t)$ and, thus, the slopes q_t^\pm depend on time t . For times much shorter than the relaxation time ($\gamma t \ll 2$), the singularities lie far away from the real axis. As time increases, the singularities move along the imaginary axis toward the real axis. Finally, for times much longer than the relaxation time ($\gamma t \gg 2$), the singularities approach limiting points: $p_1^\pm \rightarrow \pm iq_*^\pm$, which are shown in Fig. 26 by circled \times 's. Thus, as illustrated in Fig. 27, the slopes q_t^\pm monotonously decrease in time and saturate at long times:

$$q_t^\pm \rightarrow q_*^\pm = \pm p_0 + \frac{\omega_0}{\kappa\sqrt{1-\rho^2}} \quad \text{for } \gamma t \gg 2. \quad (81)$$

The slopes (81) are in agreement with Eq. (69) valid for $\gamma t \gg 2$. The time dependence q_t^\pm at short times can be also found analytically:

$$q_t^\pm \approx \pm p_0 + \sqrt{p_0^2 + \frac{4\gamma}{\kappa^2(1-\rho^2)t}} \quad \text{for } \gamma t \ll 2. \quad (82)$$

The dotted curve in Fig. 27 shows that Eq. (82) works very well for short times t , where the slope diverges at $t \rightarrow 0$.

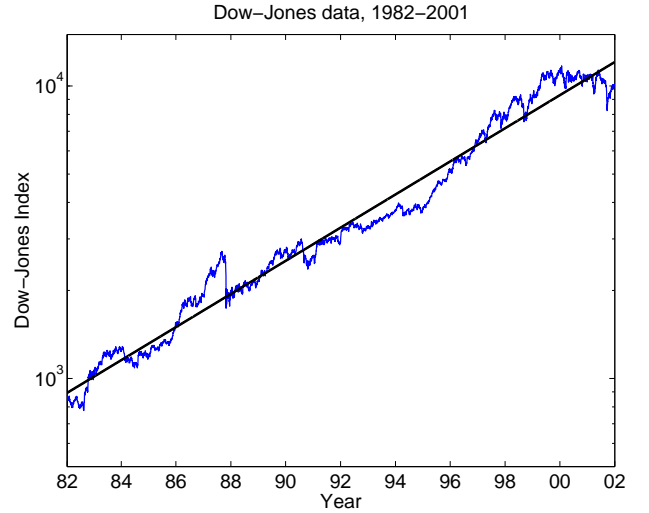


FIG. 28: Log-linear plot of the Dow-Jones versus time, for the period 1982–2001. The straight solid line through the data points represents a fit of the Dow-Jones index with an exponential function with growth rate $\mu = 13.3\%/\text{year}$.

H. Comparison with Dow-Jones time series

To test the model against financial data, we downloaded daily closing values of the Dow-Jones industrial index for the period of 20 years from 1 January 1982 to 31 December 2001 from the Web site of Yahoo⁷³. The data set contains 5049 points, which form the time series $\{S_\tau\}$, where the integer time variable τ is the trading day number. We do not filter the data for short days, such as those before holidays.

Given $\{S_\tau\}$, we use the following procedure to extract the probability density $P_t^{(DJ)}(r)$ of log-return r for a given time lag t . For the fixed t , we calculate the set of log-returns $\{r_\tau = \ln S_{\tau+t}/S_\tau\}$ for all possible times τ . Then we partition the r -axis into equally spaced bins of the width Δr and count the number of log-returns r_τ belonging to each bin. In this process, we omit the bins with occupation numbers less than five, because we consider such a small statistics unreliable. Only less than 1% of the entire data set is omitted in this procedure. Dividing the occupation number of each bin by Δr and by the total occupation number of all bins, we obtain the probability density $P_t^{(DJ)}(r)$ for a given time lag t . To find $P_t^{(DJ)}(x)$, we replace $r \rightarrow x + \mu t$. In Fig. 28 we plot the value of the Dow-Jones index, and the fit with an exponential function corresponding to an inflation rate μ . In Fig. 29 we illustrate the histogram corresponding to the probability density $P_t^{(DJ)}(r)$ for a time lag $t = 5$ days. The first and last bin in Fig. 29 show all the events outside the two vertical dashed lines. These events are very rare, contribute less than 1% to the entire number of data points, and therefore they are discarded in the fitting process.

Assuming that the system is ergodic, so that ensemble averaging is equivalent to time averaging, we compare $P_t^{(DJ)}(x)$ extracted from the time series data and $P_t(x)$ calculated in

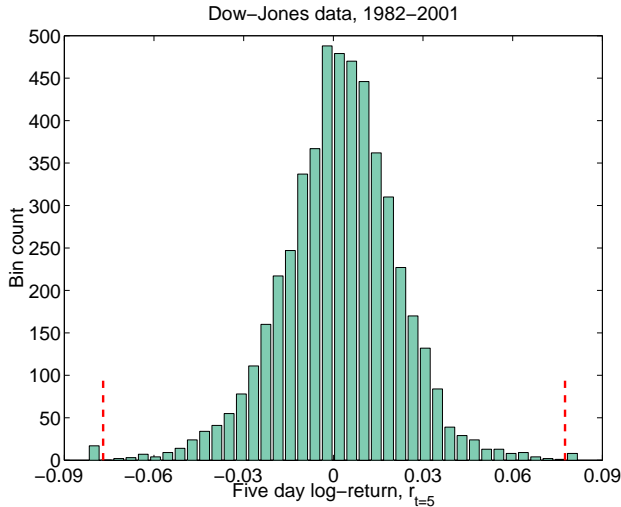


FIG. 29: Histogram of five day log-returns $r_{t=5}$. The first and the last bin, which are separated from the rest by the two vertical dashed lines, are discarded in the fitting process. The population of the first (last) bin contains all the extreme events from $-\infty(+\infty)$ to the left(right) dashed line.

previous sections, which describes ensemble distribution. In the language of mathematical statistics, we compare our theoretically derived population distribution with the sample distribution extracted from the time series data. We determine parameters of the model by minimizing the mean-square deviation $\sum_{x,t} |\ln P_t^{(DJ)}(x) - \ln P_t(x)|^2$, where the sum is taken over all available x and $t = 1, 5, 20, 40$, and 250 days. These values of t are selected because they represent different regimes: $\gamma t \ll 1$ for $t = 1$ and 5 days, $\gamma t \approx 1$ for $t = 20$ days, and $\gamma t \gg 1$ for $t = 40$ and 250 days. As Figs. 23 and 24 illustrate, our expression (57) and (58) for the probability density $P_t(x)$ agrees with the data very well, not only for the selected five values of time t , but for the whole time interval from 1 to 250 trading days. However, we cannot extend this comparison to t longer than 250 days, which is approximately 1/20 of the entire range of the data set, because we cannot reliably extract $P_t^{(DJ)}(x)$ from the data when t is too long.

The values obtained for the four fitting parameters ($\gamma, \theta, \kappa, \mu$) are given in Table III. Within the scattering of the data, we do not find any discernible difference between the fits with the correlation coefficient ρ being zero or slightly different from zero. Thus, we conclude that the correlation ρ between the noise terms for stock price and variance in Eq. (25) is practically zero, if it exists at all. Our conclusion is in contrast with the value $\rho = -0.58$ found in⁷⁴ by fitting the leverage correlation function introduced in⁷⁵. Further study is necessary in order to resolve this discrepancy. Nevertheless, all theoretical curves shown in this chapter are calculated for $\rho = 0$, and they fit the data very well.

All four parameters ($\gamma, \theta, \kappa, \mu$) shown in Table III have the dimensionality of 1/time. The first line of the Table gives their values in the units of 1/day, as originally determined in our fit. The second line shows the annualized values of the parameters

Units	γ	θ	κ	μ
1/day	4.50×10^{-2}	8.62×10^{-5}	2.45×10^{-3}	5.67×10^{-4}
1/year	11.35	0.022	0.618	0.143

TABLE III: Parameters of the model obtained from the fit of the Dow-Jones data. We also find $\rho = 0$ for the correlation coefficient and $1/\gamma = 22.2$ trading days for the relaxation time of variance.

in the units of 1/year, where we utilize the average number of 252.5 trading days per calendar year to make the conversion. The relaxation time of variance is equal to $1/\gamma = 22.2$ trading days = 4.4 weeks \approx 1 month, where we took into account that 1 week = 5 trading days. Thus, we find that variance has a rather long relaxation time, of the order of one month, which is in agreement with the conclusion of Ref.⁷⁴.

Using the numbers given in Table III, we find the value of the parameter $2\gamma\theta/\kappa^2 = 1.296$. Since this parameter is greater than one, the stochastic process (24) never reaches the domain $v < 0$, as discussed in Sec. III B.

The effective growth rate of stock prices is determined by the coordinate $r_m(t)$ where the probability density $P_t(r_m)$ is maximal. Using the relation $r_m = x_m + \mu t$ and Eq. (71), we find that the actual growth rate is $\bar{\mu} = \mu - \gamma\theta/2\omega_0 = 13\%$ per year. This number coincides with the average growth rate of the Dow-Jones index obtained by a simple fit of the time series $\{S_\tau\}$ with an exponential function of τ . The effective stock growth rate $\bar{\mu}$ is comparable with the average stock volatility after one year $\sigma = \sqrt{\theta} = 14.7\%$. Moreover, the parameter (33), which characterizes the width of the stationary distribution of variance, is equal to $\chi = 0.54$. This means that the distribution of variance is broad, and variance can easily fluctuate to a value twice greater than the average value θ . Thus, even though the average growth rate of stock index is positive, there is a substantial probability $\int_{-\infty}^0 dr P_t(r) = 17.7\%$ to have negative growth for $t = 1$ year.

According to (81), the asymmetry between the slopes of exponential tails for positive and negative x is given by the parameter p_0 , which is equal to 1/2 when $\rho = 0$ (see also the discussion of Eq. (72) at the end of Sec. III F). The origin of this asymmetry can be traced back to the transformation from (23) to (26) using Itô's formula. It produces the term $0.5v_t dt$ in the r.h.s. of (26), which then generates the second term in the r.h.s. of (28). The latter term is the only source of asymmetry in x of $P_t(x)$ when $\rho = 0$. However, in practice, the asymmetry of the slopes $p_0 = 1/2$ is quite small (about 2.7%) compared with the average slope $q_*^\pm \approx \omega_0/\kappa = 18.4$.

I. Conclusions

We derived an analytical solution for the probability distribution $P_t(x)$ of log-returns x as a function of time t for the model of a geometrical Brownian motion with stochastic variance. The final result has the form of a one-dimensional Fourier integral (57) and (58). [In the case $\rho = 0$, the equations have the simpler form (72), (73), and (74).] Numerical evaluation of the integral (57) is simple compared

with computationally-intensive numerical solution of the original Fokker-Planck PDE or Monte-Carlo simulation of the stochastic processes.

Our result agrees very well with the Dow-Jones data, as shown in Fig. 23. Comparing the theory and the data, we determine the four (non-zero) fitting parameters of the model, particularly the variance relaxation time $1/\gamma = 22.2$ days. For time longer than $1/\gamma$, our theory predicts scaling behavior (65) and (66), which the Dow-Jones data indeed exhibits over seven orders of magnitude, as shown in Fig. 24. The scaling function $P_*(z) = K_1(z)/z$ is expressed in terms of the first-order modified Bessel function K_1 . Previous estimates in literature of the relaxation time of volatility using various indirect indicators range from 1.5 days⁵⁷ (p. 80) to less than one day and more than few tens of days⁵¹ (p. 70) for S&P 500 and 73 days for the half-life of the Dow-Jones index⁵⁶. Since we have a very good fit of the entire probability distribution function for times from 1 to 250 trading days, we believe that our estimate, 22.2 days, is much more reliable. A close value of 19.6 days was found in Ref.⁷⁴.

As Fig. 23 shows, the probability distribution $P_t(x)$ is exponential in x for large $|x|$, where it is characterized by time-dependent slopes $d \ln P/dx$. The theoretical analysis presented in Sec. III G shows that the slopes are determined by the singularities of the function $F_t(p_x)$ from (58) in the complex plane of p_x that are closest to the real axis. The calculated time dependence of the slopes $d \ln P/dx$, shown in Fig. 27, agrees with the data very well, which further supports our statement that $1/\gamma = 22.2$ days. Exponential tails in the probability distribution of stock log-returns have been noticed in literature before⁵¹ (p. 61),⁷⁶, however time dependence of the slopes has not been recognized and analyzed theoretically. In Ref.⁵⁵, the power-law behavior of the tails has been emphasized. However, the data for S&P 500 were analyzed in Ref.⁵⁵ only for short time lags t , typically shorter than one day. On the other hand, our data analysis is performed for the time lags longer than one day, so the results cannot be directly compared.

Our analytical expression for the probability distribution of returns can be utilized to calculate option pricing. Notice that it is not necessary to introduce the ad-hoc function $\lambda(S, v, t)$, the market-price of risk, as is typically done in literature^{50,57,58,59,60}, because now $P_t(x)$ is known explicitly. Using the true probability distribution of returns $P_t(x)$ should improve option pricing compared with the previous efforts in literature.

Although we tested our model for the Dow-Jones index, there is nothing specific in the model which indicates that it applies only to stock market data. It would be interesting to see how the model performs when applied to other time series, for example, the foreign exchange data⁷⁷, which also seem to exhibit exponential tails.

IV. PATH-INTEGRAL SOLUTION OF THE COX-INGERSOLL-ROSS/FELLER MODEL

In this section we provide details on the path-integral solution of the variance process (24). The stochastic differential equation of the Cox-Ingwersoll-Ross/Feller process, Eq. (24), is

$$dx_t = -\gamma(x_t - \theta)dt + \kappa\sqrt{x_t}dW_t. \quad (83)$$

Here θ is the long-time mean of x , γ is the rate of relaxation to this mean, W_t is the standard Wiener process, and κ is a parameter that controls the amplitude of the noise. Eq. (83) is known in financial literature as the Cox-Ingwersoll-Ross (CIR) process and it was used to model of interest rate dynamics. Feller⁷⁹ used equation (83) to model population extinction in biological systems. Recently, the same equation (83) was used to model the thermal reversal of magnetization in a magnetic grain⁸⁰.

One quantity of interest to calculate is the conditional (transition) probability $P(x, t | x_i, t_i)$, which gives the probability to find the system at position x at time t , given that it was at position x_i at initial time t_i . The transition probability $P(x, t | x_i, t_i)$ of the stochastic process described by (83) satisfies the Fokker-Planck equation

$$\begin{aligned} \frac{\partial}{\partial t} P(x, t | x_i, t_i) &= \frac{\partial}{\partial x} [\gamma(x - \theta)P(x, t | x_i, t_i)] \\ &+ \frac{\kappa^2}{2} \frac{\partial^2}{\partial x^2} [xP(x, t | x_i, t_i)] \end{aligned} \quad (84)$$

The Fokker-Planck equation (84) can be thought of as a Schrödinger equation in imaginary (Euclidean) time written in the coordinate “x” representation,

$$\frac{\partial}{\partial t} P(x, t | x_i, t_i) = -\hat{H}(\hat{p}, \hat{x})P(x, t | x_i, t_i) \quad (85)$$

with the Hamiltonian

$$\hat{H} = \frac{\kappa^2}{2}\hat{p}^2\hat{x} - i\gamma\hat{p}(\hat{x} - \theta). \quad (86)$$

In the coordinate representation, the momentum operator \hat{p} is given by the derivative operator $\hat{p} = -id/dx$. The canonical commutation relation holds true: $[\hat{x}, \hat{p}] = i$. Using this analogy with quantum mechanics, the transition probability $P(x, t | x_i, t_i)$ can be found using the method of path integrals. The transition probability is the matrix element of the evolution operator $\hat{U}(t, t_i) = \exp(-\hat{H}(t - t_i))$ between the initial state $|x_i\rangle$, and final state $\langle x_f|$,

$$P(x_f, t_f | x_i, t_i) = \langle x_f | e^{-\hat{H}(t_f - t_i)} | x_i \rangle. \quad (87)$$

The standard construction of the path integral is obtained by splitting the time interval $[t_i, t_f]$ into M time steps of equal size $\epsilon = (t_f - t_i)/M$. One uses the multiplication property of the transition probability to write

$$\langle x_f | e^{-\hat{H}(t_f - t_i)} | x_i \rangle = \int \prod_{j=1}^{M-1} (dx_j)$$

$$\times \prod_{j=1}^M \langle x_j | e^{-\hat{H}(t_j - t_{j-1})} | x_{j-1} \rangle. \quad (88)$$

The contribution coming from interval (t_j, t_{j+1}) is evaluated as

$$\begin{aligned} \langle x_j | e^{-\hat{H}(t_j - t_{j-1})} | x_{j-1} \rangle &= \int dp_j \langle x_j | p_j \rangle \\ &\times \langle p_j | e^{-\hat{H}(t_j - t_{j-1})} | x_{j-1} \rangle. \end{aligned} \quad (89)$$

The matrix element inside the integral in Eq.(89) can be now evaluated to

$$\langle p_j | e^{-\hat{H}(t_j - t_{j-1})} | x_{j-1} \rangle \approx e^{-\epsilon H(p_j, x_{j-1})} \langle p_j | x_{j-1} \rangle. \quad (90)$$

Substitute the scalar product

$$\langle x_j | p_j \rangle = \frac{e^{ip_j x_j}}{\sqrt{2\pi}} \quad \langle p_j | x_{j-1} \rangle = \frac{e^{-ip_j x_{j-1}}}{\sqrt{2\pi}}, \quad (91)$$

and Eq.(90) back into (89), to obtain

$$\begin{aligned} P(x_f, t_f | x_i, t_i) &= \int \prod_{j=1}^{M-1} dx_j \int \prod_{j=1}^M \frac{dp_j}{2\pi} \\ &\times e^{\sum_{j=1}^M ip_j(x_j - x_{j-1}) - \epsilon H(p_j, x_{j-1})}. \end{aligned} \quad (92)$$

where

$$H(p_j, x_{j-1}) = \frac{\kappa^2}{2} p_j^2 x_{j-1} - i\gamma p_j(x_{j-1} - \theta) \quad (93)$$

By taking the limit $M \rightarrow \infty$ in Eq.(92), one arrives at the path integral expression

$$P(x_f, t_f | x_i, t_i) = \int \mathcal{D}x \mathcal{D}p e^{S[x, p]} \quad (94)$$

where the action functional $S[x_t, p_t]$ is given by

$$S[x_t, p_t] = \int_{t_i}^{t_f} dt \left[ip_t \dot{x}_t - \frac{\kappa^2}{2} p_t^2 x_t + i\gamma p_t(x_t - \theta) \right]. \quad (95)$$

The phase-space path integral from Eq.(94) has to be calculated over all continuous paths $p(t)$ and $x(t)$ satisfying the boundary conditions $x(t_i) = x_i$ and $x(t_f) = x_f$.

For most path-integrals in physics, the path integral is quadratic in momenta and because of that it is customary to integrate first the momenta $p(t)$ to obtain the Lagrangean of the problem, and be left with the path integral over the coordinate $x(t)$. This route can be taken here too, but the resulting Lagrangean will have a position dependent mass, which unnecessary complicates the remaining integration over the coordinate. It is important to notice that the problem is linear in the coordinate $x(t)$ and quadratic in $p(t)$, so the original Schrödinger formulation will be simpler in the momentum representation. In the path-integral formulation, it turns out that the integration over $x(t)$ is trivial and gives a delta functional.

Both the continuous expression (94) and the discrete one (92) have their own computational advantages. In the following, I will use the discrete form (92), because for this problem, it allows for a quick and transparent solution. The exponent in (92) can be rearranged in the form

$$\begin{aligned} S &= i(p_M x_f - p_0 x_i) - i\epsilon\gamma\theta \sum_{j=1}^M p_j \\ &+ i \sum_{j=1}^{M-1} x_j \left[(p_{j-1} - p_j) + \epsilon\gamma p_j + i\epsilon \frac{\kappa^2}{2} p_j^2 \right] \end{aligned} \quad (96)$$

where I made the notation $p_0 = p_1 - \epsilon(\gamma p_1 + i\kappa^2 p_1^2/2)$.

The path integral over the coordinate can be taken one by one, starting with the one over dx_{M-1} . The result is a delta function $2\pi\delta(p_{M-1} - p_M + \epsilon\gamma p_M + i\epsilon\kappa^2 p_M^2/2)$. The integration over p_{M-1} resolves the delta function for the value of p_{M-1} equal to $p_{M-1} \equiv (1 - \epsilon\hat{T})p_M$, where the operator $\hat{T} = \gamma(\cdot) + k^2(\cdot)^2/2$. The integral over dx_{M-2} is done next, with the result $2\pi\delta(p_{M-2} - (1 - \epsilon\hat{T})^2 p_M)$, followed by the integral over dp_{M-2} . The procedure is repeated until the last pair $dx_1 dp_1$. In this way we get $p_0 = (1 - \epsilon\hat{T})p_1 = (1 - \epsilon\hat{T})^M p_M$.

The value of the transition probability is

$$P(x_f, t_f | x_i, t_i) = \int_{-\infty}^{\infty} \frac{dp_M}{2\pi} e^{i(p_M x_f - p_0 x_i) - i\epsilon\gamma\theta \sum_{j=1}^M p_j} \quad (97)$$

where in (97), $p_j \equiv (1 - \epsilon\hat{T})^{(M-j)} p_M$ for $j = \overline{0, M}$. Because of the approximation used in (90), Eq.(97) is valid only when the number of time splittings $M \rightarrow \infty$. In this limit we have

$$\frac{p_j - p_{j-1}}{\epsilon} = \hat{T} p_j \quad \longrightarrow \quad \frac{dp_t}{dt} = \hat{T} p_t \quad \text{with} \quad p(t_f) = p_M \quad (98)$$

The differential equation $dp_t/dt = \hat{T} p_t = \gamma p_t + i\frac{\kappa^2}{2} p_t^2$ is a Bernoulli equation and has the solution

$$p_t = \frac{1}{(\frac{1}{p_M} + \frac{i\kappa^2}{2\gamma}) e^{-\gamma(t-t_f)} - \frac{i\kappa^2}{2\gamma}}. \quad (99)$$

The expression for the transition probability in the $M \rightarrow \infty$ limit is

$$P(x_f, t_f | x_i, t_i) = \int_{-\infty}^{\infty} \frac{dp_M}{2\pi} e^{i(p_M x_f - p_0 x_i) - i\gamma\theta \int_{t_i}^{t_f} dt p_t} \quad (100)$$

where p_t is given by Eq.(99). The time integral in (100) can be evaluated as

$$\int_{t_i}^{t_f} dt p_t = -\frac{2i}{\kappa^2} \int_0^{\gamma T} \frac{dy}{\zeta e^y - 1} = -\frac{2i}{\kappa^2} \ln \frac{\zeta - e^{-\gamma T}}{\zeta - 1} \quad (101)$$

where

$$\zeta = 1 - \frac{2i\gamma}{\kappa^2 p_M}, \quad \text{and} \quad T = t_f - t_i. \quad (102)$$

After minor rearrangements in the argument of the logarithm, the final result is given in the form of a Fourier integral

$$P(x_f, t_f | x_i, t_i) = \int_{-\infty}^{\infty} \frac{dp_M}{2\pi} e^{i(p_M x_f - p_0 x_i)}$$

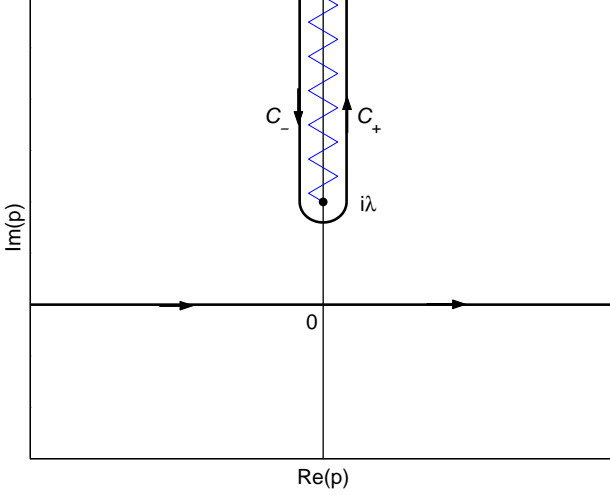


FIG. 30: The complex plane of p . The branch cut due to the denominator of Eq. (106) is shown as a broken line. The contour \mathcal{C} has been deformed so that it encircles the branch cut.

$$\times \exp \left\{ -\frac{2\gamma\theta}{\kappa^2} \ln \left[1 + \frac{i\kappa^2}{2\gamma} (1 - e^{-\gamma T}) p_M \right] \right\} \quad (103)$$

where

$$p_0 \equiv p(t = t_i) = \frac{p_M e^{-\gamma T}}{1 + \frac{i\kappa^2}{2\gamma} (1 - e^{-\gamma T}) p_M} \quad (104)$$

Although, the integral from Eq.(103) seems complicated, it can be evaluated exactly by integration in the complex plane. Introduce the following notations

$$\nu = 2\gamma\theta/\kappa^2, \quad \text{and} \quad \lambda = 2\gamma/\kappa^2(1 - \exp(-\gamma T)). \quad (105)$$

The integral in (103) becomes

$$P(x_f, t_f | x_i, t_i) = \int_{-\infty}^{+\infty} \frac{dp}{2\pi} \frac{\exp \left\{ ipx_f - i \frac{pe^{-\gamma T}}{1+ip/\lambda} x_i \right\}}{(1+ip/\lambda)^\nu} \quad (106)$$

There is a branch point singularity in the complex plane of p which is situated on the imaginary axis, for $p = i\lambda$. We take the branch cut to extend from $i\lambda$ to $i\infty$. For positive x_f , the contour of integration is deformed so that it encircles the branch cut. The complex plane of p , and the contour of integration are presented in FIG.30. The contribution from the contour \mathcal{C} can be split into two parts, one from the part to the left of the cut \mathcal{C}_- and the other part, to the right of the cut \mathcal{C}_+ . The Bessel function $J_\nu(z)$ has the following integral representation due to Schläfli

$$J_\nu(z) = \frac{1}{2\pi i} \left(\frac{z}{2}\right)^\nu \int_{-\infty}^{(0+)} dt t^{-\nu-1} e^{t-z^2/4t}, \quad (107)$$

where the integral is taken along a contour around the branch cut on the negative real axis, encircling it in the counterclockwise direction. By making the change of variable $p \rightarrow -ip$ in (106), the transition probability $P(x_f, t_f | x_i, t_i)$ can be expressed in terms of the Bessel function as

$$P(x_f, t_f | x_i, t_i) = \lambda^\nu e^{-\lambda(x_f + x_i e^{-\gamma T})} \times \left(-\frac{x_i}{x_f} \lambda^2 e^{-\gamma T} \right)^{\frac{1-\nu}{2}} J_{\nu-1}(2i\sqrt{x_i x_f \lambda^2 \exp(-\gamma T)}). \quad (108)$$

The modified Bessel function $I_\nu(z)$ is defined in terms of the usual Bessel function $J_\nu(z)$ of imaginary argument by the relation

$$I_\nu(z) = e^{-\frac{i\pi\nu}{2}} J_\nu(e^{i\pi/2} z) \quad \text{for} \quad -\pi < \arg(z) \leq \pi/2. \quad (109)$$

This relation allows to write **the final result** as

$$P(x_f, t_f | x_i, t_i) = \lambda^\nu e^{-\lambda(x_f + x_i e^{-\gamma T})} \times \left(\frac{x_i}{x_f} \lambda^2 e^{-\gamma T} \right)^{\frac{1-\nu}{2}} I_{\nu-1}(2\sqrt{x_i x_f \lambda^2 \exp(-\gamma T)}), \quad (110)$$

were λ and ν are given by (105), and $T = t_f - t_i$.

The normalization of the probability density,

$$\int_0^\infty dx_f P(x_f, t_f | x_i, t_i) = 1,$$

can be proved easily by making use of the result

$$\int_0^\infty dx x^{\nu+1} e^{-\alpha x^2} I_\nu(\beta x) = \frac{\beta^\nu}{(2\alpha)^{\nu+1}} e^{\beta^2/4\alpha}. \quad (111)$$

We can check the validity of expression (110) by taking several limiting cases:

- In the limit $T \rightarrow \infty$, the transition probability $P(x_f, t_f | x_i, t_i)$ should become the stationary probability distribution (given in our paper). The argument of the Bessel function from (110) goes to zero in the limit $T \rightarrow \infty$. The modified Bessel function $I_\nu(z)$ has the following small argument behavior

$$I_\mu(z) \approx \frac{1}{\Gamma(\mu+1)} \left(\frac{z}{2}\right)^\mu \quad \text{for} \quad z \rightarrow 0^+. \quad (112)$$

Substituting the expression (112) into (110), we obtain

$$P(x_f, t_f | x_i, -\infty) \equiv P_*(x_f) = \frac{\lambda^\nu}{\Gamma(\nu)} x_f^{\nu-1} e^{-\lambda x_f}. \quad (113)$$

which is the stationary distribution.

- In the short time limit, $T \rightarrow 0$ ($\lambda \rightarrow \infty$), the probability distribution should approach a delta function, $P(x_f, t_f | x_i, t_i) = \delta(x_f - x_i)$. The argument of the Bessel function from (110) goes to infinity in the limit $T \rightarrow 0$. The modified Bessel function $I_\nu(z)$ has the following large argument behavior

$$I_\mu(z) \approx \frac{e^z}{\sqrt{2\pi z}} \quad \text{for} \quad z \rightarrow \infty \quad (114)$$

Substituting (114) back into (110), we obtain

$$P(x_f, t_f | x_i, t_i) = f(x_i/x_f) \lim_{\lambda \rightarrow \infty} \sqrt{\frac{\lambda}{4\pi x_i}} e^{-\lambda(\sqrt{x_f} - \sqrt{x_i})^2} = \delta(x_f - x_i) \quad (115)$$

[†] Email:adrian.dragulescu@constellation.com

- ¹ J. D. Farmer, Computing in Science and Engineering **1**, #6, p. 26 (1999); R. N. Mantegna and H. E. Stanley, *An Introduction to Econophysics* (Cambridge University Press, Cambridge, 2000).
- ² G. H. Wannier, *Statistical Physics* (Dover, New York, 1987).
- ³ It is also implied that the system is extensive. We study only extensive models, so the nonextensive generalization of entropy by C. Tsallis, J. Stat. Phys. **52**, 479 (1988); Braz. J. Phys. **29**, 1 (1999) is not relevant for our consideration.
- ⁴ D. M. Mueth, H. M. Jaeger, and S. R. Nagel, Phys. Rev. E **57**, 3164 (1998); M. L. Nguyen and S. N. Coppersmith, Phys. Rev. E **59**, 5870 (1999).
- ⁵ M. Shubik, in *The Economy as an Evolving Complex System II*, edited by W. B. Arthur, S. N. Durlauf, and D. A. Lane (Addison-Wesley, Reading, 1997) p. 263.
- ⁶ S. Ispolatov, P. L. Krapivsky, and S. Redner, Eur. Phys. J. B **2**, 267 (1998).
- ⁷ C. R. McConnell and S. L. Brue, *Economics: Principles, Problems, and Policies* (McGraw-Hill, New York, 1996).
- ⁸ E. W. Montroll and M. F. Shlesinger, Proc. Natl. Acad. Sci. USA **79**, 3380 (1982); O. Malcai, O. Biham, and S. Solomon, Phys. Rev. E **60**, 1299 (1999); D. Sornette and R. Cont, J. Phys. I (France) **7**, 431 (1997); J.-P. Bouchaud and M. Mézard, cond-mat/0002374.
- ⁹ E. M. Lifshitz and L. P. Pitaevskii, *Physical Kinetics* (Pergamon Press, New York, 1993).
- ¹⁰ A. Chakraborti and B. K. Chakrabarty, Eur. Phys. J. B. **17** 167 (2000).
- ¹¹ Martin Shubik, *The Theory of Money and Financial Institutions*, vol. 2 (The MIT Press, Cambridge, 1999), p. 192.
- ¹² P. Bak, S. F. Nørrelykke, and M. Shubik, Phys. Rev. E **60**, 2528 (1999).
- ¹³ Masanao Aoki, *New Approaches to Macroeconomic Modeling* (Cambridge University Press, Cambridge, 1996).
- ¹⁴ V. Pareto, *Cours d'Economie Politique* (Lausanne, 1897).
- ¹⁵ G.F. Shirras, Economic Journal **45**, 663 (1935).
- ¹⁶ B. Mandelbrot, Internat. Economic Review **1**, 79 (1960).
- ¹⁷ N. Kakwani, *Income Inequality and Poverty* (Oxford University Press, Oxford, 1980).
- ¹⁸ F. Levy, Science **236**, 923 (1987).
- ¹⁹ R. Gibrat, *Les Inégalités Economique* (Sirely, Paris, 1931).
- ²⁰ E.W. Montroll, M.F. Shlesinger, J. Stat. Phys. **32**, 209 (1983).
- ²¹ M. Kalecki, Econometrica **13**, 161 (1945).
- ²² M. Levy, S. Solomon, Int. J. Mod. Phys. C **7**, 595 (1996); D. Sornette, R. Cont, J. Phys. I (France) **7**, 431 (1997).
- ²³ The U.S. Census data, <http://ferret.bls.census.gov/>.
- ²⁴ The PSID Web site, <http://www.isr.umich.edu/src/psid/>.
- ²⁵ *Statistics of Income—1997, Individual Income Tax Returns*, Pub. 1304, Rev. 12-99 (IRS, Washington DC, 1999)
See http://www.irs.ustreas.gov/prod/tax_stats/soi/.
- ²⁶ P. Sailer, M. Weber, *Household and Individual Income Data from Tax Returns* (IRS, Washington DC, 1998), <http://ftp.fedworld.gov/pub/irs-soi/petas98.pdf>.
- ²⁷ T. Petska, M. Strudler, R. Petska, *Further Examination of the Distribution of Individual Income and Taxes Using a Consistent and Comprehensive Measure of Income* (IRS, 2000), <http://ftp.fedworld.gov/pub/irs-soi/disindit.exe>.
- ²⁸ W. Feller, *An Introduction to Probability Theory and Its Applications*, vol. 2 (John Wiley, New York, 1966) p. 10.
- ²⁹ D.H. Weinberg, *A Brief Look at Postwar U.S. Income Inequality*, P60-191 (Census Bureau, Washington, 1996), <http://www.census.gov/hhes/www/p60191.html>.
- ³⁰ *1040: Forms and Instructions* (IRS, Washington, 1999).
- ³¹ H.F. Lydall, Econometrica **27**, 110 (1959).
- ³² Zhi-Feng Huang, S. Solomon, cond-mat/0103170; S. Solomon, P. Richmond, cond-mat/0102423, Physica A **299**, 1 (2001).
- ³³ J.-P. Bouchaud, M. Mezard, Physica A **282**, 536 (2000).
- ³⁴ D. Sornette, R. Cont, J. Phys. I (France) **7**, 431 (1997).
- ³⁵ A. A. Drăgulescu, V. M. Yakovenko, Eur. Phys. J. B. **20**, 585 (2001).
- ³⁶ A. A. Drăgulescu, V. M. Yakovenko, Eur. Phys. J. B **17**, 723 (2000).
- ³⁷ M. Levy, S. Solomon, Physica A **242**, 90 (1997).
- ³⁸ Distribution of Personal Wealth, Inland Revenue, <http://www.inlandrevenue.gov.uk/stats/distribution2000.pdf>.
- ³⁹ Personal Incomes, Inland Revenue, 1998-99: Table 3.3 of <http://www.inlandrevenue.gov.uk/stats/>, file income2000.pdf. For 1997-98: http://www.inlandrevenue.gov.uk/stats/table3_3a.htm.
- ⁴⁰ Annual Abstract of Statistics, Office of National Statistics, <http://www.statistics.gov.uk>.
- ⁴¹ T. Cranshaw, Pareto, Poverty and Riches, unpublished.
- ⁴² Individual Tax Statistics by States in 1998, IRS, http://www.irs.gov/tax_stats/soi/ind_st.html, file 98IN54CM.EXE.
- ⁴³ P. W. Anderson, in *The Economy as an Evolving Complex System* (Reading, MA, Addison-Wesley, 1988).
- ⁴⁴ W. Souma, cond-mat/0011373.
- ⁴⁵ The Interactive Currency Table, <http://www.xe.net/ict/>.
- ⁴⁶ S. Abe and Y. Okamoto (Eds.) *Nonextensive Statistical Mechanics and its Applications*, (Springer-Verlag, Berlin, 2001)
- ⁴⁷ G. Kaniadakis and A. M. Scarfone, Physica A **305**, 69 (2002).
- ⁴⁸ B. Milanovic, World Bank Working Paper 2244, (1999), <http://www.worldbank.org/poverty/inequal/abstracts/recent.htm>.
- ⁴⁹ A. A. Drăgulescu and V. M. Yakovenko, <http://arXiv.org/abs/cond-mat/0203046>.
- ⁵⁰ P. Wilmott, *Derivatives* (John Wiley & Sons, New York, 1998).
- ⁵¹ J. P. Bouchaud and M. Potters, *Theory of Financial Risks* (Cambridge University Press, Cambridge, 2001).
- ⁵² R. N. Mantegna and H. E. Stanley, *An Introduction to Econophysics* (Cambridge University Press, Cambridge, 2000).
- ⁵³ J. Voit, *The Statistical Mechanics of Financial Markets* (Springer, Berlin, 2001).
- ⁵⁴ B. B. Mandelbrot, Journal of Business **36**, 393 (1963).
- ⁵⁵ R. N. Mantegna and H. E. Stanley, Nature **376**, 46 (1995); P. Gopikrishnan, M. Meyer, L. A. N. Amaral, and H. E. Stanley, European Physical Journal B **3**, 139 (1998); P. Gopikrishnan, V. Plerou, L. A. N. Amaral, M. Meyer, and H. E. Stanley, Physical Review E **60**, 5305 (1999).
- ⁵⁶ R. F. Engle and A. J. Patton, Quantitative Finance **1**, 237 (2001).
- ⁵⁷ J. P. Fouque, G. Papanicolaou, and K. R. Sircar, *Derivatives in Financial Markets with Stochastic Volatility* (Cambridge University Press, Cambridge, 2000); International Journal of Theoretical and Applied Finance, **3**, 101 (2000).
- ⁵⁸ J. Hull and A. White, Journal of Finance **42**, 281 (1987); C. A. Ball and A. Roma, Journal of Financial and Quantitative Analysis **29**, 589 (1994); R. Schöbel and J. Zhu, European Finance Review **3**, 23 (1999).
- ⁵⁹ E. M. Stein and J. C. Stein, Review of Financial Studies **4**, 727 (1991).
- ⁶⁰ S. L. Heston, Review of Financial Studies **6**, 327 (1993).

- ⁶¹ B. E. Baaquie, *Journal de Physique I* (France) **7**, 1733 (1997).
- ⁶² R. Courant and D. Hilbert, *Methods of Mathematical Physics, vol. 2* (John Wiley & Sons, New York, 1962).
- ⁶³ R. P. Feynman and A. R. Hibbs, *Quantum Mechanics and Path Integrals* (McGraw-Hill, New York, 1965).
- ⁶⁴ L. S. Schulman, *Techniques and Application of Path Integration* (John Wiley & Sons, New York, 1981).
- ⁶⁵ H. Kleinert, *Path Integrals in Quantum Mechanics, Statistics, and Polymer Physics* (World Scientific, Singapore, 1995).
- ⁶⁶ E. Bennati, M. Rosa-Clot, and S. Taddei, *International Journal of Theoretical and Applied Finance* **2**, 381 (1999).
- ⁶⁷ D. G. McMillan, *Applied Economics Letters* **8**, 605 (2001).
- ⁶⁸ R. G. Tompkins, *Journal of Futures Markets* **21**, 43 (2001); Y.-N. Lin, N. Strong, and X. Xu, *Journal of Futures Markets* **21**, 197 (2001); G. Fiorentini, A. Leon, and G. Rubio, *Journal of Empirical Finance*, to be published.
- ⁶⁹ C. W. Gardiner, *Handbook of Stochastic Methods for Physics, Chemistry, and the Natural Sciences* (Springer-Verlag, Berlin, 1993).
- ⁷⁰ C. M. Bender and S. A. Orszag, *Advanced Mathematical Methods for Scientists and Engineers* (Springer-Verlag, New York, 1999).
- ⁷¹ Y. Liu, P. Gopikrishnan, P. Cizeau, M. Meyer, C.-K. Peng, and H. E. Stanley, *Physical Review E* **60**, 1390 (1999).
- ⁷² I. S. Gradshteyn and I. R. Ryzhik, *Table of Integrals, Series, and Products* (Academic Press, New York, 1996), formula 3.914.
- ⁷³ Yahoo Finance <http://finance.yahoo.com/>. To download data, type in the symbol box: “DJI”, and then click on the link: “Download Spreadsheet”.
- ⁷⁴ J. Masoliver and J. Perelló, preprints <http://lanl.arXiv.org/abs/cond-mat/0111334> and <http://lanl.arXiv.org/abs/cond-mat/0202203>.
- ⁷⁵ J.-P. Bouchaud, A. Matacz, and M. Potters, *Physical Review Letters* **87**, 228701 (2001).
- ⁷⁶ L. C. Miranda and R. Riera, *Physica A* **297**, 509 (2001).
- ⁷⁷ R. Friedrich, J. Peinke and C. Renner, *Physical Review Letters* **84**, 5254 (2000); C. Renner, J. Peinke and R. Friedrich, *Physica A* **298**, 499 (2001).
- ⁷⁸ J. C. Cox, J. E. Ingersoll, S. A. Ross *The Journal of Business*, **52**, No. 1, 51 (1979).
- ⁷⁹ W. Feller, *The Annals of Mathematics, 2nd Ser.*, **54**, No. 1, 173 (1951).
- ⁸⁰ V. L. Safonov, *Journal of Applied Physics*, **85**, No. 8, 4370 (1999).
- ⁸¹ The infinitesimal increments of the Wiener process dW_t are normally distributed (Gaussian) random variables with zero mean and the variance equal to dt .
- ⁸² An attempt to determine the probability distribution of volatility empirically for the S&P 500 stock index was done in Ref.⁷¹.